# Age–Energy Tradeoff in Random-Access Poisson Networks

Fangming Zhao, Xinghua Sun, *Member, IEEE*, Wen Zhan, *Member, IEEE*, Xijun Wang, *Member, IEEE*, Jie Gong, *Member, IEEE*, and Xiang Chen, *Member, IEEE*

***Abstract*—Energy efficiency and Age of Information (AoI) are two key performance metrics for many emerging battery-limited fresh-aware IoT networks, where random access protocols, such as Aloha, are usually adopted. Yet, in large-scale random access scenarios, the energy efficiency and AoI performance would degrade severely if the network is not configured properly. This paper aims to address this issue by studying the performance limit of energy efficiency under AoI constraint and how to achieve such limit in a slotted Aloha-based Poisson bipolar network. Specifically, we evaluate the energy efficiency via the lifetime throughput, which is defined as the number of update packets successfully decoded by the receiver during the lifetime of each transmitter. The explicit expression of the lifetime throughput is derived, based on which the maximum lifetime throughput with or without AoI constraint and the corresponding optimal channel access probability and packet arrival rate are characterized. The analysis reveals that both the maximum lifetime throughput and AoI-optimal lifetime throughput decline as the node density increases, while the gap between them would be non-negligible if the power ratio of the transmission state and the waiting state is large. Further with AoI constraint, it is shown that the AoI-constrained maximum lifetime throughput has to be sacrificed if the constraint is stringent. The effects of key system parameters on the optimal network configurations and age-energy tradeoff are also discussed, which provide important insights on practical battery-limited fresh-aware IoT network design.**

***Index Terms*—Energy efficiency, age of information, random access, lifetime throughput, Aloha.**

Manuscript received 11 April 2022; revised 30 August 2022; accepted 20 September 2022. Date of publication 27 September 2022; date of current version 22 November 2022. This work was supported in part by the Key-Area Research and Development Program of Guangdong Province under Grant 2019B010158001; in part by the National Natural Science Foundation of China under Grant 62001524, Grant 62271513, and Grant 62171481; in part by the Guangdong Basic and Applied Basic Research Foundation under Grant 2021A1515012631; and in part by the Shenzhen Science and Technology Program under Grant RCBS20210706092408010 and Grant 2021A04. This article was presented in part at the IEEE Wireless Communications and Networking Conference (WCNC), April 2022 [DOI: 10.1109/WCNC51071.2022.9771861]. The editor coordinating the review of this article was P. Manzoni. *(Corresponding authors: Xinghua Sun; Wen Zhan.)*

Fangming Zhao, Xinghua Sun, and Wen Zhan are with the School of Electronics and Communication Engineering, Sun Yat-sen University (Shenzhen Campus), Shenzhen 518107, China (e-mail: zhaofm@mail2.sysu.edu.cn; sunxinghua@mail.sysu.edu.cn; zhanw6@mail.sysu.edu.cn).

Xijun Wang and Xiang Chen are with the School of Electronics and Information Technology, Sun Yat-sen University, Guangzhou 510006, Guangdong, China (e-mail: wangxijun@mail.sysu.edu.cn; chenxiang@mail.sysu.edu.cn).

Jie Gong is with the School of Computer Science and Engineering, Sun Yat-sen University, Guangzhou 510006, Guangdong, China (e-mail: gongj26@mail.sysu.edu.cn).

Digital Object Identifier 10.1109/TGCN.2022.3210138

## I. Introduction

The INTERNET-OF-THINGS (IoT) paradigm has found wide applications in various domains such as real-time monitoring [2], intelligent transportation [3], industrial control [4], and healthcare [5]. Energy efficiency and the information freshness are two critical performance metrics for these IoT applications, such as the forest fire warning system, in which battery-limited sensors are placed in remote areas for monitoring the forest fire. High energy efficiency is required to support a long battery lifetime of each IoT node. Meanwhile, the information reporting needs to be timely.

With the densely-deployed low-cost IoT nodes and the desire for ubiquitous connectivity, random access schemes, such as Aloha, were usually adopted as the medium access protocol for numerous IoT nodes to share spectrum sources [6] distributed nature of the behavior of each node, severe interference occurs that deteriorates the energy efficiency and information freshness. Considering the explosive growth of the number of IoT devices [7], there is an urgent need to study how to optimize the energy efficiency and information freshness in large-scale random access IoT networks.

### A. Energy Efficiency Optimization

Energy efficiency is always a key concern in wireless network design. Extensive studies have been focused on improving the energy efficiency of random access IoT networks by reducing the channel contention [8], [9], [10], [11], [12], sleep scheduling [9], [13], [14], power control [15], [16], and rational idle listening [17]. It was pointed out in [18] that for the battery-operated IoT devices, a large body of the energy consumption was wasted in the failure transmissions due to packet collision. Reference [9] formulated a new CSMA-based scheme that combines both throughput optimality and energy efficiency by tuning the back-off and sleep timers to reduce the collision. Reference [11] proposed n-phase CSMA/CA that provides a tunable trade-off between energy efficiency, delay, and spectral efficiency. The energy-optimum channel access rate for the underwater Aloha network has been derived in [12].

The classic collision model was adopted in these studies, where one node can successfully access the channel if and only if there are no concurrent transmissions. Yet, key effects of physical attributes in wireless channels such as fading, path loss, and interference were ignored. To remedy this, the stochastic geometry along with capture model, i.e., a packet can be successfully decoded as long as its received Signal to Interference plus Noise Ratio (SINR) is above a certain threshold, were adopted in [13], [19], [20]. Specifically, [19] evaluated the energy efficiency-spectral efficiency tradeoff in heterogeneous network with sleep control. Energy efficiency of multi-tier cellular networks has been analyzed in [20]. Through the deployment of sleep strategies and small cells, the power consumption minimization and energy efficiency maximization problems in cellular network has been investigated in [13]. However, these studies focus on cellular network scenarios, and the large-scale random access network deserves further study. Moreover, in large-scale network, the evolution of queues associated with the transmitters are coupled with each other over space and time via the interference they cause. Therefore, we will combine the queuing theory and stochastic geometry to characterize the space-time interaction among queues and optimize the energy efficiency of the large-scale IoT networks.

### B. *Age of Information Optimization*

To measure the timeliness of the information, Age of Information (AoI), defined as the time elapsed since the latest packet has been delivered, was proposed in [21] and has drawn wide attention in the existing literature. Extensive studies have been conducted to optimize the AoI performance with energy constraint. For instance, various works considered energy harvest sources with finite or infinite battery capacity [22], [23], [24], [25]. By proposing various types of information updating policies, such as the lazy updating policy [26], the monotone threshold policy [27], and the optimal online status policy [28], the average AoI performance was optimized with constraints on energy harvest rate. However, these studies only focused on a point-to-point communication scenario. In practice, IoT networks generally consist of many nodes that intend to communicate with their destinations via shared spectrum, which usually constitutes a multiple access network. In IoT networks with massive traffic links, severe interference may incur, leading to energy efficiency and AoI degradation.

There have been studies of the AoI performance on large-scale random access IoT networks by combining queuing theory and stochastic geometry [29], [30], [31], [32], [33], [34], which, however, assume nodes are without battery limitation. For instance, in our recent work [29], a spatiotemporal analytical framework was proposed for Poisson bipolar random access network with infinite battery capacity. Explicit expressions of minimum peak AoI and corresponding optimal channel access probability and packet arrival rate were obtained. Yet, if the battery limitation is further considered, then how to satisfy the AoI QoS requirement remains largely unknown.

### C. *Age-Energy Tradeoff Optimization*

The tradeoff between the energy efficiency and the classical performance metrics has been extensively studies in [35], [36], [37], including spectrum efficiency, throughput, and delay and so on. Recently, the age-energy tradeoff draws much attention. For age-energy tradeoff in the point-to-point scenario, the analysis in [38], [39], [40], [41] has revealed that the optimization of one metric is usually achieved at the cost of the other.

Evaluating the energy-age tradeoff in a large-scale random access IoT network is much more challenging than that in the point-to-point case, as queueing status of neighboring nodes coupled with each other due to the broadcast nature of the wireless channel and the lack of a central controller. Reference [42] aimed at AoI-constrained energy efficiency optimization in the sensor network. However, the channel error probability was assumed to be unrelated to the interference among nodes. The interference was considered in [43] while the scenario is limited to a two-node case. An energy cost minimization [44] and sampling cost minimization [45] with average AoI constraints have been studied, yet the formulation only captures channel fading and the noise. In short, the above works ignored or idealized key physical attributes in wireless systems, e.g., the interference of co-channel transmitters and node distribution. Thus, it remains largely unknown how those factors affect the age-energy tradeoff and how to perform the AoI-constrained energy efficiency optimization in large-scale distributed network.

### D. *Our Contribution*

This paper aims to address above open issues in a large-scale Aloha-based Poisson bipolar network, where each transmitter associates with a receiver and accesses the channel with a certain probability at each time slot. With a finite amount of energy, the life of a transmitter comes to an end if its energy runs out. Accordingly, the number of successfully-transmitted packets during the lifetime of each transmitter, which is termed as lifetime throughput, is limited. A larger lifetime throughput indicates better energy efficiency. Based on the spatio-temporal analytical framework in our previous work [29], which was established by combining the stochastic geometry and queueing theory, we derive the explicit expression of the lifetime throughput of each node, where the physical attributes, i.e., the interference, channel fading and the node distribution density, are taken into consideration. We aim to obtain the optimal channel access probability and packet arrival rate for maximizing the lifetime throughput while satisfying the AoI constraint, where peak AoI is adopted as the metric for information freshness. The individual channel access probability optimization has been investigated in our earlier work [1]. Both the individual optimization and joint optimization are further considered in this paper. Our main contributions are summarized below.

- We derive close-form expressions of the maximum lifetime throughput and the corresponding optimal transmission parameters without AoI constraint. Using these expressions, we find that, in the individual optimization case, when the Power Ratio of the Transmission State and the Waiting State (PRTW) or the node deployment density is small, the optimal channel access probability (resp. the optimal packet arrival rate) equals one, and a large packet arrival rate (resp. a large channel access rate) always improves the maximum lifetime throughput. Otherwise, the maximum lifetime throughput is not

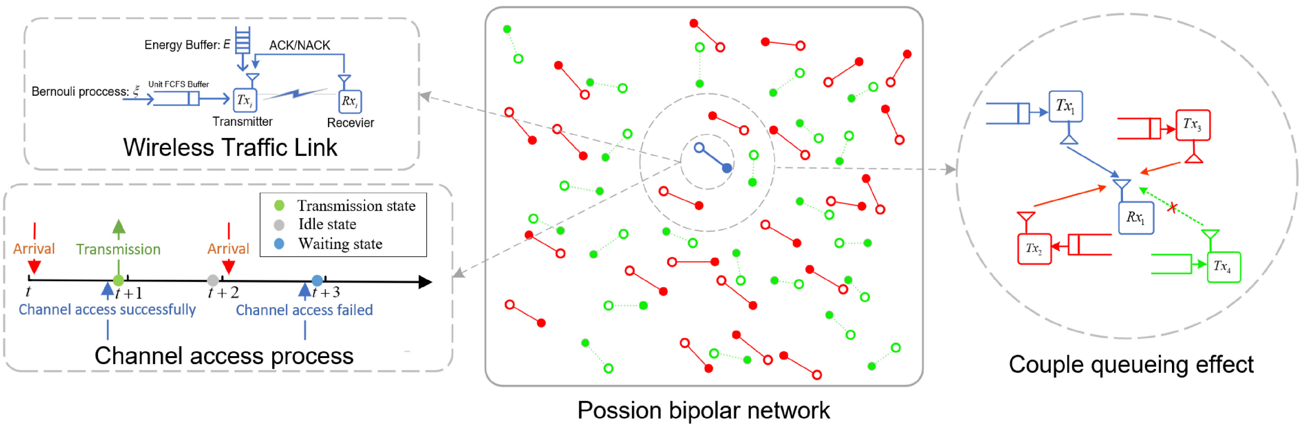


Fig. 1. Snapshot of Poisson bipolar network in consideration. The up-left figure illustrates the queueing model of a generic transmitter. The down-left figure illustrates the channel access process and corresponding states. The right figure shows the coupling effect among queues.

sensitive to a large packet arrival rate (resp. a large channel access probability) due to the limit of the packet arrival rate of the data queue (resp. channel access probability); in the joint tuning case, the maximum lifetime throughput can be achieved by either reducing the packet arrival rate or the channel access probability for interference management when PRTW is large.

- We further investigate the energy-age tradeoff. Specifically, the AoI-constrained maximum lifetime throughput and the corresponding optimal channel access probability and packet arrival rate are characterized in both individual optimization and joint optimization cases. The results indicate that when the network interference is not significant, the lifetime throughput performance and peak AoI performance both benefit from frequent updates and transmissions. When the network interference is severe, the lifetime throughput and peak AoI can be optimized simultaneously only in some special cases, such as PRTW equals one with individual optimization. Otherwise, the gap between the maximum lifetime throughput and the AoI-optimal lifetime throughput enlarges as the PRTW increases, revealing a crucial energy-age tradeoff.
- We also study the effect of the peak AoI constraint on the optimal parameter settings. It is revealed that when the PRTW is large, the feasible region of the optimal parameters can be divided into two parts depending on the peak AoI constraint. When the peak AoI constraint is not stringent, the optimal parameters are determined by the PRTW instead of the peak AoI constraint; Otherwise, the optimal parameters depend on the peak AoI constraint and are insensitive to the PRTW. The network suffers from lifetime throughput loss.

The rest of the paper is organized as follows. Section II presents the system model and derivation of the lifetime throughput. The lifetime throughput with/without peak AoI constraint is optimized by tuning the channel access probability and packet arrival rate, respectively, in Section III and Section IV. Section V further extends the analysis into the joint optimization case. Finally, Section VI summarizes the work.

TABLE I
MAIN NOTATIONS

| Notations | Definition |
|---|---|
| $q$ | Channel access probability |
| $\xi$ | Packet arrival rate |
| $p$ | Probability of successful transmission |
| $\lambda$ | Node deployment density |
| $R$ | Distance between transmitter and receiver |
| $\gamma$ | SNR at the receiver end |
| $\theta$ | Decoding SINR threshold |
| $\alpha$ | Path-loss fading coefficient |
| $M$ | Lifetime throughput |
| $A_p$; $\bar{A}_p$ | Peak Age of Information; Peak Age of Information constraint |
| $P_T$; $P_W$; $P_I$ | Power consumption in the transmission, waiting and idle states |
| $T_S$; $T_F$; $T_W$; $T_I$ | Time period in the success, failure, waiting and idle states |

## II. System Model and Preliminary Analysis

### A. Spatial-Temporal Scenario

Consider a mobile device-to-device (D2D) network scenario[1] which can be modeled as a Poisson bipolar network. As Fig. 1 illustrates, transmitters are scattered according to a homogeneous Poisson point process (PPP) of density $\lambda$. The main notations used throughout this article are summarized in Table I. Each transmitter is paired with a receiver that is situated in distance $R$ and oriented at a random direction. In this network, the time is slotted into equal-length

[1]Typical examples of AoI-aware energy-sensitive D2D networks include industrial wireless networks (IWNs) [46]. D2D communications are used for proximity transmissions due to numerous vicinal sensor-actuator pairs [46]. Differing from small-cell techniques (e.g., femtocell and picocell), D2D communications with random access protocol allows devices to directly communicate with each other with minimum coordination under less involvement of the base station, leading to extremely low power consumption and signaling overhand. The information freshness and energy efficiency are critical to IWNs. For example, in oil refineries, spilling of oil tanks can be avoided by timely monitoring of oil level, and the senors for status update are usually deployed in inaccessible or hazardous regions with limited energy resources.

intervals and the transmission of each packet lasts for one slot. The packets arrive at each transmitter following independent Bernoulli processes of mean rate $\xi$. We assume each transmitter is equipped with a unit-size buffer and hence a newly incoming packet will be dropped if the buffer is full. At the end of each time slot, transmitters with non-empty buffers will access the channel with a fixed channel access probability $q$.

### B. Probability of Successful Transmission

In this paper, we consider the Rayleigh fading channel and denote path-loss exponent as $\alpha > 2$. All nodes share the same spectrum. Due to the broadcast nature of the wireless channel, each node's transmission would cause interference to others. Consider a packet is successfully delivered if the received SINR exceeds a decoding threshold $\theta$, i.e.,

$$p_i(t) = P(\mathrm{SINR}_i(t) > \theta). \tag{1}$$

We assume a high mobility random walk model for the positions of transmitters. Therefore, the received $\mathrm{SINR}_i(t)$ of each transmitter $i$, $i \in \mathbb{N}$, can be considered as i.i.d. across time $t$. By symmetry, the probability of successful transmission is also identical across all the transmitters. To that end, we drop the indices $i$ and $t$ in (1) and denote $p$ as the probability of successful transmission, which has been obtained in [29] as

$$p = \exp\left\{-\frac{\lambda\pi\theta^{\frac{2}{\alpha}}R^2}{\mathrm{sinc}\left(\frac{2}{\alpha}\right)}\frac{q\xi}{\xi + pq(1-\xi)} - \theta R^{\alpha}\gamma^{-1}\right\}, \tag{2}$$

where $\gamma$ is the SNR at the receiver. In the following, we let $c = \pi\theta^{\frac{2}{\alpha}}/\mathrm{sinc}(\frac{2}{\alpha})$ for simplicity. The dynamics of packet transmissions over each wireless link can be regarded as a Geo/Geo/1/1 queue with the service rate $qp$.

### C. Age of Information

Age of information captures the timeliness of information delivered at the receiver side. The definition of this metric is given below [33].

*Definition 1 (Age of Information):* Consider a typical transmitter-receiver pair. Let $\{G(t_i)\}_{i\geq 1}$ be the sequence of generation times of information packets that were delivered and $\{t_i\}_{i\geq 1}$ be the corresponding times at which these packets are received at the destination. Amongst the packets received till time $t$, denote the index of the latest generated one by $n_t = \arg\max_i\{G(t_i)|t_i \leq t\}$. The age of information at the receiver is defined as $\Delta(t) = t - G(t_{n_t})$

This definition implies that a packet containing fresher information can bring in more AoI reduction. Therefore, we assume the buffer size of each node is one to reduce the waiting time in the queue, and keep the information fresh. In this paper, we leverage the peak AoI $A_p$ as a metric to quantify the timeliness of information, which is defined as the time average of age values at time instants when there is a packet transmitted successfully. The peak AoI $A_p$ in the considered scenario has been obtained in [29] as

$$A_p = \frac{1}{\xi} + \frac{2}{qp} - 1. \tag{3}$$

### D. Lifetime Throughput

Different from that in [29], we assume that each transmitter has a finite amount of initial energy $E$, and thus the life of a transmitter comes to an end if its energy runs out. Since each transmitter has the same configuration, the expected lifetime of each transmitter is identical, which is denoted as $T$ in unit of time slots. During the lifetime, each transmitter could be in the following four states: 1) idle state, i.e., the queue is empty; 2) waiting state, i.e., the queue is not empty, yet the node does not transmit; 3) successful transmission state, i.e., the packet transmission is successful; 4) failure state, i.e., the packet transmission fails. Note that no matter the transmission is successful or not, the amount of energy consumption for that transmission is identical. Let $T_I$, $T_W$, $T_S$, $T_F$ denote the expected number of time slots for each node being in the idle, waiting, successful transmission and failure states during its lifetime, respectively, and $P_I$, $P_W$, $P_T$ denote the energy consumption in the idle, waiting and transmission states, respectively, in unit of time slot, where we assume $P_I = P_W$. In this paper, we are interested in lifetime throughput $M$, which is defined as the total number of update packets successfully decoded by the receiver during the lifetime of each transmitter. Appendix A reveals that

$$M = \rho qpT = \frac{E\xi qp}{P_W(1-q)\xi + P_I qp(1-\xi) + P_T q\xi}, \tag{4}$$

where $\rho = \frac{\xi}{\xi+qp-\xi qp}$ is the non-empty probability of each transmitter's queue [29], $\rho qp$ is the network throughput in Geo/Geo/1/1 case and $E$ denotes the initial amount of energy at each transmitter. It can be seen from (4) that the lifetime throughput $M$ is the product of the throughput and the lifetime length $T$. Both of them depend on channel access probability $q$ and the packet arrival rate $\xi$ according to (2). Intuitively, a higher channel access probability may increase the output of the traffic link, but it also shortens the lifetime due to higher power consumption. A similar phenomenon occurs as the packet arrival rate increases. Accordingly, how to tune the channel access probability $q$ and the packet arrival rate $\xi$ for optimizing the lifetime throughput performance is of great interest. We aim to maximize the lifetime throughput $M$ by tuning the channel access probability $q$ and the packet arrival rate $\xi$. We further consider the constraint that the peak AoI $A_p$ is expected to be no larger than a certain threshold $\bar{A}_p$. We then have the optimization problem

$$\begin{aligned} M^* = &\max_{q\in(0,1],\ \xi\in(0,1]} \quad M \\ &\quad \mathrm{s.t.} \quad A_p \leq \bar{A}_p. \end{aligned} \tag{5}$$

Before looking into the joint tuning problem in (5), we would first decompose (5) into two sub-optimization problems: optimal tuning of channel access probability $q$ for a fixed $\xi$, and optimal tuning of the packet arrival rate $\xi$ for a fixed $q$, because joint tuning of channel access probability and the packet arrival rate might be infeasible in some practical scenarios. For instance, the packet arrival rate is usually determined by the applications. For the power grid state reporting in smart grid, the mean reporting period is set to be every 15 minutes [48], which indicates that a new packet arrives at the queue in every 15 minutes.

## III. Optimal Tuning of Channel Access Probability

Given the packet arrival rate $\xi$, Theorem 1 presents the optimal channel access probability[2] $q_\xi^*$ that maximizes the lifetime throughput $M$, i.e., $M_\xi^* = \max_q\ M$.

[2]The optimal tuning of the channel channel access probability depends on the statistical traffic information (such as the node density), instead of the realtime number of active nodes requesting transmission in each time slot. Tracking and estimating the time-varying number of active nodes could be highly challenging and energy-consuming.

### A. Lifetime Throughput Optimization Without Constraint

Let us first examine the case when $\bar{A}_p \to \infty$, i.e., the age constraint is released. According to Theorem 1, the maximum lifetime throughput $M_\xi^{*,\bar{A}_p\to\infty}$ is given by (12), shown at the bottom of the next page, which is achieved when the optimal channel access probability $q_\xi^{*,\bar{A}_p\to\infty}$ is set to be (13), shown at the bottom of the next page. Fig. 2 demonstrates how the optimal channel access probability $q_\xi^{*,\bar{A}_p\to\infty}$ and the corresponding maximum lifetime throughput $M_\xi^{*,\bar{A}_p\to\infty}$ vary with

*Theorem 1:* With $A_p \le \bar{A}_p$, the maximum lifetime throughput $M_\xi^*$ is given by

$$M_\xi^* = \begin{cases} \dfrac{2E\xi}{P_W\left(\bar{A}_p+1-\frac{1}{\xi}-\left(\bar{A}_p-1+\frac{1}{\xi}\right)q_{\min}\right)+P_T q_{\min}}, & \text{if } \lambda c R^2 > \dfrac{[\xi+p_*(1-\xi)]^2}{\xi^2\frac{P_T}{P_W}+p_*\xi(1-\xi)} \text{ and } A_p^{q=q_{\xi,\mathrm{AoI}}^*} \le \bar{A}_p \le A_p^{q=q_\xi^{*,\bar{A}_p\to\infty}}, \\ \dfrac{\frac{E}{P_W}\exp\left\{-\frac{2}{1+\sqrt{1+\frac{4}{\lambda c R^2}\left(\frac{P_T}{P_W}-1\right)}}-\theta R^\alpha\gamma^{-1}\right\}}{\frac{\lambda c R^2}{2}\left(1+\sqrt{1+\frac{4}{\lambda c R^2}\left(\frac{P_T}{P_W}-1\right)}\right)+\left(\frac{P_T}{P_W}-1\right)}, & \text{if } \lambda c R^2 > \dfrac{[\xi+p_*(1-\xi)]^2}{\xi^2\frac{P_T}{P_W}+p_*\xi(1-\xi)} \text{ and } \bar{A}_p \ge A_p^{q=q_\xi^{*,\bar{A}_p\to\infty}}, \\ \dfrac{Ep_*\xi}{P_W p_*(1-\xi)+P_T\xi}, & \text{if } \lambda c R^2 \le \dfrac{[\xi+p_*(1-\xi)]^2}{\xi^2\frac{P_T}{P_W}+p_*\xi(1-\xi)} \text{ and } \bar{A}_p \ge A_p^{q=q_{\xi,\mathrm{AoI}}^*}, \\ \text{no solution}, & \text{otherwise}. \end{cases} \tag{6}$$

The corresponding optimal channel access probability $q_\xi^*$ is given by

$$q_\xi^* = \begin{cases} \mathbb{W}_0\left(-\frac{2\lambda c R^2\xi\exp\left\{\theta R^\alpha\gamma^{-1}\right\}}{2(1-\xi)+\xi\left(\bar{A}_p-\frac{1}{\xi}+1\right)}\right)\Big/\left(-\frac{\lambda c R^2\xi\left(\bar{A}_p-\frac{1}{\xi}+1\right)}{2(1-\xi)+\xi\left(\bar{A}_p-\frac{1}{\xi}+1\right)}\right), & \text{if } \lambda c R^2 > \frac{[\xi+p_*(1-\xi)]^2}{\xi^2\frac{P_T}{P_W}+p_*\xi(1-\xi)} \text{ and } A_p^{q=q_{\xi,\mathrm{AoI}}^*} \le \bar{A}_p \le A_p^{q=q_\xi^{*,\bar{A}_p\to\infty}}, \\ \dfrac{1}{\left(\frac{\lambda c R^2}{2}\left(1+\sqrt{1+\frac{4}{\lambda c R^2}\left(\frac{P_T}{P_W}-1\right)}\right)-\frac{1-\xi}{\xi}\exp\left\{-\frac{2}{1+\sqrt{1+\frac{4}{\lambda c R^2}\left(\frac{P_T}{P_W}-1\right)}}-\theta R^\alpha\gamma^{-1}\right\}\right)}, & \text{if } \lambda c R^2 > \frac{[\xi+p_*(1-\xi)]^2}{\xi^2\frac{P_T}{P_W}+p_*\xi(1-\xi)} \text{ and } \bar{A}_p \ge A_p^{q=q_\xi^{*,\bar{A}_p\to\infty}}, \\ 1, & \text{if } \lambda c R^2 \le \frac{[\xi+p_*(1-\xi)]^2}{\xi^2\frac{P_T}{P_W}+p_*\xi(1-\xi)} \text{ and } \bar{A}_p \ge A_p^{q=q_{\xi,\mathrm{AoI}}^*}, \\ \text{no solution} & \text{otherwise}. \end{cases} \tag{7}$$

In (6), we have

$$q_{\min} = \frac{\mathbb{W}_0\left(-\dfrac{2\lambda c R^2\xi\exp\left\{\theta R^\alpha\gamma^{-1}\right\}}{2(1-\xi)+\xi\left(\bar{A}_p-\frac{1}{\xi}+1\right)}\right)}{-\dfrac{\lambda c R^2\xi\left(\bar{A}_p-\frac{1}{\xi}+1\right)}{2(1-\xi)+\xi\left(\bar{A}_p-\frac{1}{\xi}+1\right)}}, \tag{8}$$

where $\mathbb{W}_0(\cdot)$ represents the principal branch of the Lambert *W* function [49]; $p_*$ is the probability of successful transmission when $q=1$ and can be obtained from the following equation

$$p_* = \exp\left\{-\lambda c R^2\frac{\xi}{\xi+p_*(1-\xi)} - \theta R^\alpha\gamma^{-1}\right\}. \tag{9}$$

$A_p^{q=q_{\xi,\mathrm{AoI}}^*}$ is the minimum peak AoI without energy constraint and has been derived in [29] as

$$A_p^{q=q_{\xi,\mathrm{AoI}}^*} = \begin{cases} 2\lambda c R^2\exp\left\{\theta R^\alpha\gamma^{-1}+1\right\}-\frac{1}{\xi}+1, & \text{if } \lambda c R^2 > 1+\frac{p_*(1-\xi)}{\xi}, \\ \frac{1}{\xi}+\frac{2}{p_*}-1, & \text{otherwise}, \end{cases} \tag{10}$$

and $A_p^{q=q_\xi^{*,\bar{A}_p\to\infty}}$ is the peak AoI when optimal lifetime throughput is achieved, which is given by

$$A_p^{q=q_\xi^{*,\bar{A}_p\to\infty}} = \left(\lambda c R^2\left(1+\sqrt{1+\frac{4}{\lambda c R^2}\left(\frac{P_T}{P_W}-1\right)}\right)\right)\left(\exp\left\{\frac{-2}{\sqrt{1+\left(\frac{4}{\lambda c R^2}\left(\frac{P_T}{P_W}-1\right)\right)}}-\theta R^\alpha\gamma^{-1}\right\}\right). \tag{11}$$

*Proof:* See Appendix B ■

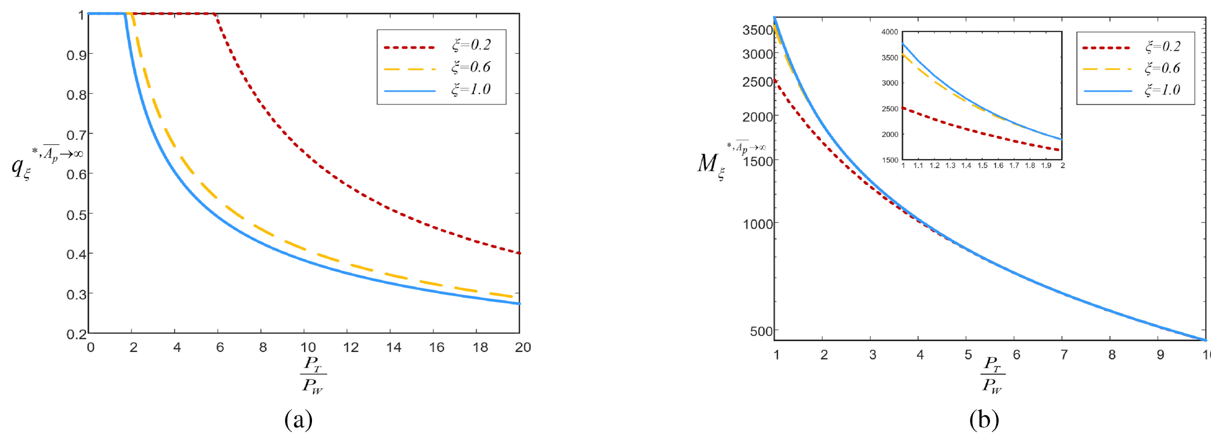


Fig. 2. Optimal channel access probability $q_\xi^{*,\bar{A}_p\to\infty}$ and the corresponding maximum lifetime throughput $M_\xi^{*,\bar{A}_p\to\infty}$ versus the PRTW $\frac{P_T}{P_W}$. $E = 2*10^4 J$, $P_W = 1\ W$, $\lambda = 0.01$, $\alpha = 3$, $\gamma = 20$, $R = 3$, $\xi \in \{0.2, 0.6, 1\}$. (a) $q_\xi^{*,\bar{A}_p\to\infty}$ versus $\frac{P_T}{P_W}$. (b) $M_\xi^{*,\bar{A}_p\to\infty}$ versus $\frac{P_T}{P_W}$.

the PRTW $\frac{P_T}{P_W}$ under different values of the packet arrival rate $\xi$. It is clear from Fig. 2a that $q_\xi^{*,\bar{A}_p\to\infty} = 1$ when $\frac{P_T}{P_W}$ is small, indicating that each transmitter should transmit at each time slot due to a low energy consumption in the transmission state. As $\frac{P_T}{P_W}$ increases, $q_\xi^{*,\bar{A}_p\to\infty}$ decreases. Similarly, the optimal channel access probability also decreases as the packet arrival rate $\xi$ increases, as Fig. 2a illustrates.

Moreover, from Fig. 2b, we observe that when $\frac{P_T}{P_W}$ is small, a larger arrival rate always leads to a better $M_\xi^{*,\bar{A}_p\to\infty}$. When $\frac{P_T}{P_W}$ increases, it is interesting to see that $M_\xi^{*,\bar{A}_p\to\infty}$ is not sensitive to the packet arrival rate $\xi$ and becomes solely dependent on $\frac{P_T}{P_W}$. This is because, in this case, the optimal channel access probability is low, with which a newly-incoming packet would often be discarded since it sees a full buffer. Thus, the increment of the arrival rate is not helpful for improving the maximum lifetime throughput.

### B. Age-Energy Optimization Tradeoff

Recall that, without energy constraint, the channel access probability can be tuned to optimize the peak AoI performance [29]. We have the optimal channel access probability $q_{\xi,\text{AoI}}^{*} = \arg\min_q A_p = \min\{\frac{1}{\lambda c R^2 - \frac{1-\xi}{\xi}\exp\{-\theta R^\alpha \gamma^{-1} - 1\}}, 1\}$.

*Corollary 1:* The optimal channel access probability for peak AoI optimization $q_{\xi,\text{AoI}}^{*}$ and the optimal channel access probability for lifetime throughput optimization $q_\xi^{*,\bar{A}_p\to\infty}$ satisfy

$$q_\xi^{*,\bar{A}_p\to\infty} \le q_{\xi,\text{AoI}}^{*}. \tag{14}$$

*Proof:* See Lemma 2 in Appendix B. ■

That is, with energy constraint, each transmitter should access the channel less frequently to alleviate the channel contention so as to reduce energy consumption, which, nevertheless, may lead to a large queueing delay and poor AoI performance. A tradeoff between lifetime throughput and peak AoI optimization is clearly indicated.

To evaluate the tradeoff, Fig. 3 further illustrates how the optimal channel access probability $q_\xi^{*,\bar{A}_p\to\infty}$ and the corresponding maximum lifetime throughput $M_\xi^{*,\bar{A}_p\to\infty}$ vary

$$M_\xi^{*,\bar{A}_p\to\infty} = \begin{cases} \dfrac{\frac{E}{P_W}\exp\left\{-\frac{2}{1+\sqrt{1+\frac{4}{\lambda c R^2}\left(\frac{P_T}{P_W}-1\right)}}-\theta R^\alpha\gamma^{-1}\right\}}{\frac{\lambda c R^2}{2}\left(1+\sqrt{1+\frac{4}{\lambda c R^2}\left(\frac{P_T}{P_W}-1\right)}\right)+\left(\frac{P_T}{P_W}-1\right)}, & \text{if } \lambda c R^2 > \frac{[\xi+p_*(1-\xi)]^2}{\xi^2\frac{P_T}{P_W}+p_*\xi(1-\xi)}, \\ \dfrac{E p_*\xi}{P_W p_*(1-\xi)+P_T\xi}, & \text{otherwise}. \end{cases} \tag{12}$$

$$q_\xi^{*,\bar{A}_p\to\infty} = \begin{cases} \dfrac{1}{\frac{\lambda c R^2}{2}\left(1+\sqrt{1+\frac{4}{\lambda c R^2}\left(\frac{P_T}{P_W}-1\right)}\right)-\frac{1-\xi}{\xi}\exp\left\{-\frac{2}{1+\sqrt{1+\frac{4}{\lambda c R^2}\left(\frac{P_T}{P_W}-1\right)}}-\theta R^\alpha\gamma^{-1}\right\}}, & \text{if } \lambda c R^2 > \frac{[\xi+p_*(1-\xi)]^2}{\xi^2\frac{P_T}{P_W}+p_*\xi(1-\xi)}, \\ 1, & \text{otherwise}. \end{cases} \tag{13}$$

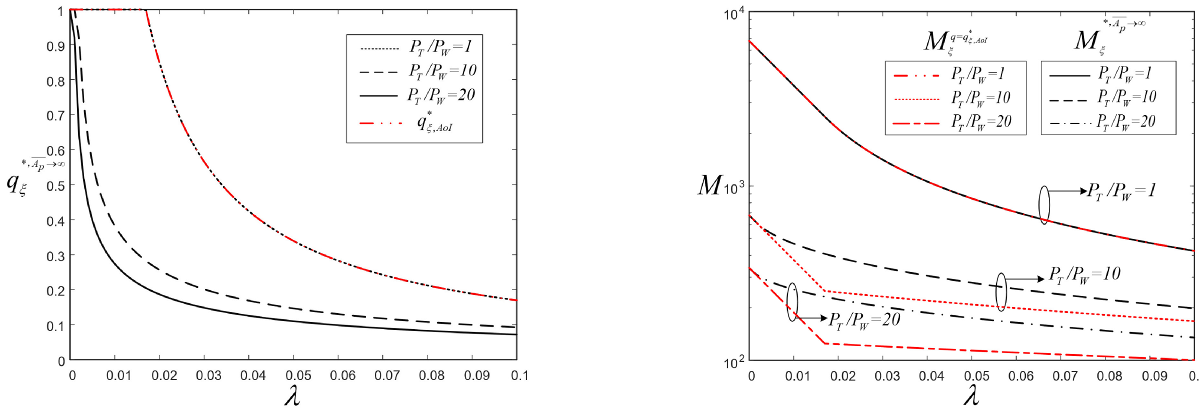


(a) (b)

Fig. 3. Optimal channel access probability $q_\xi^{*,\bar{A}_p\to\infty}$ and the lifetime throughput $M_\xi^{*,\bar{A}_p\to\infty}$, $M^{q=q^*_{\xi,\text{AoI}}}$ versus the node density $\lambda$. $E = 2*10^4 J$, $P_W = 1\ W$, $\lambda = 0.01$, $\alpha = 3$, $\gamma = 20$, $R = 3$, $\xi = 1$, $\frac{P_T}{P_W} \in \{1, 10, 20\}$. (a) $q^{*,\bar{A}_p\to\infty}$ versus $\lambda$. (b) $M_\xi^{*,\bar{A}_p\to\infty}$, $M^{q=q^*_{\xi,\text{AoI}}}$ versus $\lambda$.

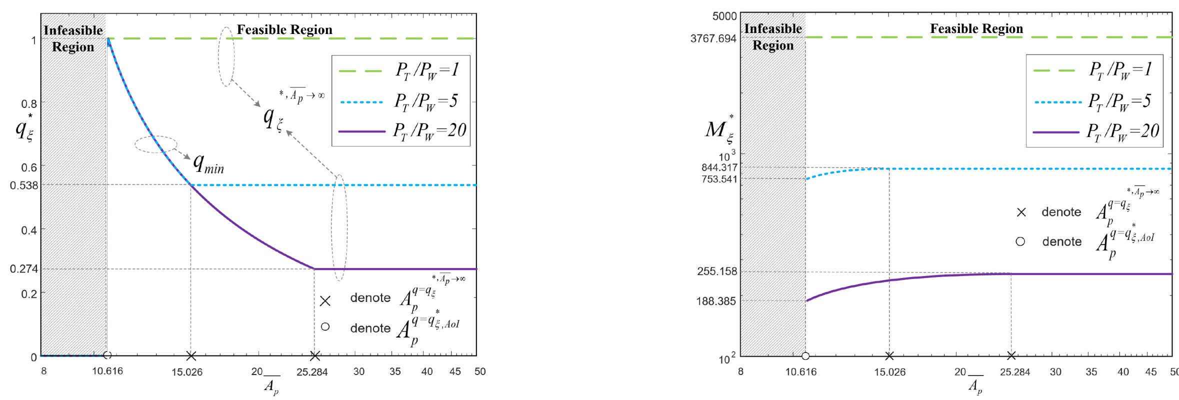


(a) (b)

Fig. 4. Optimal channel access probability $q_\xi^*$ and the corresponding maximum lifetime throughput $M_\xi^*$ versus the timeliness constraint $\bar{A}_p$. $E = 2*10^4 J$, $P_W = 1\ W$, $\lambda = 0.01$, $\alpha = 3$, $\gamma = 20$, $R = 3$, $\xi = 1$, $\frac{P_T}{P_W} \in \{1, 5, 20\}$.

with the node density $\lambda$ under different values of the PRTW $\frac{P_T}{P_W}$. Note that the optimal channel access probability for AoI optimization, i.e., $q = q^*_{\xi,\text{AoI}}$, and the corresponding energy efficiency $M_\xi^{q=q^*_{\xi,\text{AoI}}}$ are also presented in Fig. 3. The analysis reveals that both the maximum lifetime throughput and AoI-optimal lifetime throughput decline as the node deployment density increases due to mounting interference. We can see that when $\frac{P_T}{P_W} = 1$, we have $q^*_{\xi,\text{AoI}} = q_\xi^{*,\bar{A}_p\to\infty}$, and $M_\xi^{q=q^*_{\xi,\text{AoI}}} = M_\xi^{*,\bar{A}_p\to\infty}$, indicating that $M$ and $A_p$ can be optimized simultaneously. Furthermore, in Fig. 3b, as $\frac{P_T}{P_W}$ increases, the gap between the curves of $M_\xi^{*,\bar{A}_p\to\infty}$ and $M_\xi^{q=q^*_{\xi,\text{AoI}}}$ increases, implying a noticeable tradeoff between the energy efficiency optimization and AoI optimization. The reason is that the higher energy consumption in transmission state leads the nodes more careful in transmitting a packet to improve the probability of successful transmission, which makes the waiting time longer. Therefore, there is a significant difference in the optimal parameters between peak AoI and lifetime throughput and cause the performance gap between $M_\xi^{*,\bar{A}_p\to\infty}$ and $M_\xi^{q=q^*_{\xi,\text{AoI}}}$.

### C. Peak-AoI-Constrained Lifetime Throughput Optimization

With a finite peak AoI constraint $\bar{A}_p < \infty$, Fig. 4 presents the optimal channel access probability and the corresponding maximum lifetime throughput. Depending on whether the AoI-constrained lifetime throughput maximization problem in (5) has solution or not, we mark the infeasible region and the feasible region in Fig. 4.

We can see from Fig. 4 that the network falls into the infeasible region if $\bar{A}_p$ is too small. Otherwise, the network is in the feasible region, in which case the optimal channel access probability crucially depends on $\frac{P_T}{P_W}$. With $\frac{P_T}{P_W} = 1$, the optimal channel access probability $q^*_\xi = 1$ regardless of $\bar{A}_p$; When $\frac{P_T}{P_W} > 1$, as shown in Fig. 4a, the feasible region can be further partitioned into two parts, i.e., (1) $q^*_\xi = q_{\min}$

when $\bar{A}_p \leq A_p^{q=q_\xi^{*,\bar{A}_p\to\infty}}$; (2) $q_\xi^* = q_\xi^{*,\bar{A}_p\to\infty}$ when $\bar{A}_p > A_p^{q=q_\xi^{*,\bar{A}_p\to\infty}}$. In case (1), the optimal channel access probability $q_\xi^*$ decreases as $\bar{A}_p$ increases. As we have shown in Fig. 2, a lower access probability is required to optimize $M$. When the AoI constraint further looses and $\bar{A}_p$ exceeds $A_p^{q=q_\xi^{*,\bar{A}_p\to\infty}}$, $q_\xi^*$ is solely determined by $\frac{P_T}{P_W}$, which is consistent with the analysis in Fig. 2. Similar observation can also be obtained in Fig. 4b, where the constrained maximum lifetime throughput becomes insensitive to the constraint $\bar{A}_p$ when $\bar{A}_p$ is large.

## IV. Optimal Tuning of Packet Arrival Rate

Given the channel access probability $q$, Theorem 2 presents the optimal packet arrival rate $\xi_q^*$ that maximizes the AoI-constrained lifetime throughput $M$, i.e., $M_q^* = \max_\xi M$ under the peak AoI constraint.

### A. Lifetime Throughput Optimization Without Constraint

Let us first examine the case when $\bar{A}_p \to \infty$, where we have $\xi_{\min} \to 0$ and $\xi_{\max} = 1$. The maximum lifetime throughput $M_q^{*,\bar{A}_p\to\infty}$ is given by (20), shown at the bottom of the next page, which is achieved when the packet

*Theorem 2:* With $A_p \leq \bar{A}_p$, $M_q^*$ is achieved when the packet arrival rate $\xi$ is set to be

$$\xi_q^* = \begin{cases} 1, & \text{if } \lambda c R^2 < \min\left\{\frac{1}{\left(\frac{P_T}{P_W}-1\right)q^2+q}, \frac{1}{2q}\right\} \text{ and } \bar{A}_p \geq A_p^{\xi=\xi_{q,\mathrm{AoI}}^*}, \\ \xi_{\min}, & \text{if } q > \frac{1}{\frac{P_T}{P_W}-1},\ \lambda c R^2 > \frac{1}{\left(\frac{P_T}{P_W}-1\right)q^2+q} \text{ and } A_p^{\xi=\xi_{q,\mathrm{AoI}}^*} \leq \bar{A}_p \leq A_p^{\xi=\xi_q^{*,\bar{A}_p\to\infty}}, \\ \xi_{\max}, & \text{if } q < \frac{1}{\frac{P_T}{P_W}-1},\ \lambda c R^2 > \frac{1}{2q} \text{ and } A_p^{\xi=\xi_{q,\mathrm{AoI}}^*} \leq \bar{A}_p \leq A_p^{\xi=\xi_q^{*,\bar{A}_p\to\infty}}, \\ \frac{2q\exp\left\{-\frac{2}{1+\sqrt{1+\frac{4}{\lambda c R^2}\left(\frac{P_T}{P_W}-1\right)}}-\theta R^\alpha\gamma^{-1}\right\}}{\lambda c R^2 q\left(1+\sqrt{1+\frac{4}{\lambda c R^2}\left(\frac{P_T}{P_W}-1\right)}\right)+2q\exp\left\{-\frac{2}{1+\sqrt{1+\frac{4}{\lambda c R^2}\left(\frac{P_T}{P_W}-1\right)}}-\theta R^\alpha\gamma^{-1}\right\}-2}, & \text{if } \lambda c R^2 > \max\left\{\frac{1}{\left(\frac{P_T}{P_W}-1\right)q^2+q}, \frac{1}{2q}\right\} \\ & \text{and } \bar{A}_p \geq A_p^{\xi=\xi_q^{*,\bar{A}_p\to\infty}}, \\ \text{no solution}, & \text{otherwise}. \end{cases} \tag{15}$$

In (15), $\xi_{\min}$ and $\xi_{\max}$ can be obtained from the following equation

$$\xi = \left(\bar{A}_p + 1 - \frac{2}{q}\exp\left\{\lambda c R^2 q \frac{\bar{A}_p - \frac{1-\xi}{\xi}}{\bar{A}_p + \frac{1-\xi}{\xi}} + \theta R^b\gamma^{-1}\right\}\right)^{-1}. \tag{16}$$

In particular, if $\bar{A}_p < A_p^{\xi=\xi_{q,\mathrm{AoI}}^*}$, then (16) has not root and the problem has not feasible solution; if $\bar{A}_p > A_p^{\xi=1}$, then (16) has one root, which is $\xi_{\min}$, and $\xi_{\max} = 1$; if $A_p^{\xi=\xi_{q,\mathrm{AoI}}^*<1} < \bar{A}_p \leq A_p^{\xi=1}$, then (16) has two roots, i.e., $\xi_{\min}$ and $\xi_{\max}$, where $\xi_{\min} < \xi_{\max}$. In (15), $A_p^{\xi=\xi_{q,\mathrm{AoI}}^*}$ is the minimum peak AoI without energy constraint and can be expressed as

$$A_p^{\xi=\xi_{q,\mathrm{AoI}}^*} = \begin{cases} \frac{q\lambda c R^2\left(\sqrt{1+\frac{4}{q\lambda c R^2}}+1\right)+2}{2q\exp\left\{-\frac{2}{\sqrt{1+\frac{4}{q\lambda c R^2}}+1}-\theta R^\alpha\gamma^{-1}\right\}}, & \text{if } \lambda c R^2 > \frac{1}{2q}, \\ \frac{2}{q}\exp\left\{\lambda c R^2 q + \theta R^\alpha\gamma^{-1}\right\}, & \text{otherwise}. \end{cases} \tag{17}$$

$A_p^{\xi=\xi_q^{*,\bar{A}_p\to\infty}}$ is the peak AoI when optimal lifetime throughput is achieved, which is given by

$$A_p^{\xi=\xi_q^{*,\bar{A}_p\to\infty}} = \frac{1}{2q}\left(\lambda c R^2\left(1+\sqrt{1+\frac{4}{\lambda c R^2}\left(\frac{P_T}{P_W}-1\right)}\right)+2\right)\left(\exp\left\{\frac{2}{1+\sqrt{1+\frac{4}{\lambda c R^2}\left(\frac{P_T}{P_W}-1\right)}}+\theta R^\alpha\gamma^{-1}\right\}\right). \tag{18}$$

$A_p^{\xi=1}$ in (15) is the peak AoI when $\xi = 1$ and can be expressed as

$$A_p^{\xi=1} = \frac{2}{q}\exp\left\{\lambda c R^2 q + \theta R^\alpha\gamma^{-1}\right\}. \tag{19}$$

The corresponding optimal lifetime throughput $M_q^*$ can be obtained by combining (4) and (15).

*Proof:* See Appendix C. ∎

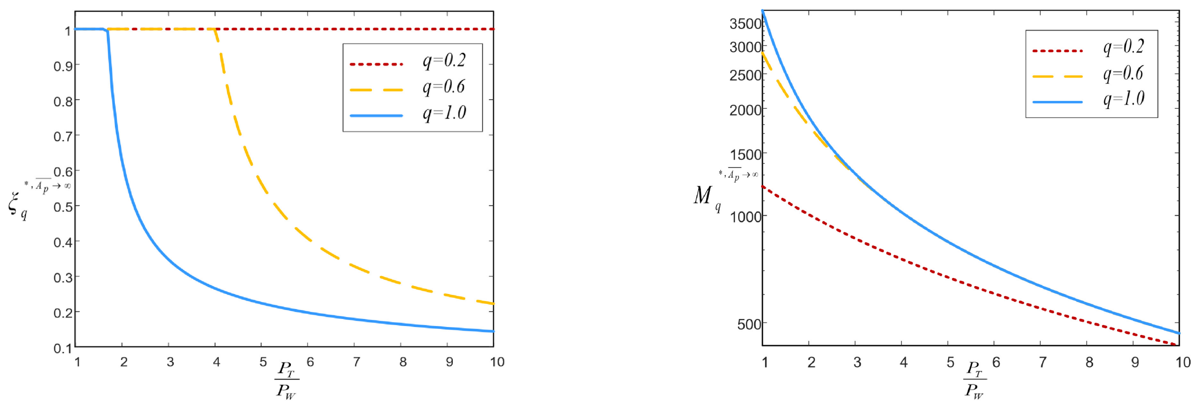


(a) (b)

Fig. 5. Optimal packet arrival rate $\xi_q^{*,\bar{A}_p\to\infty}$ and the corresponding maximum lifetime throughput $M_q^{*,\bar{A}_p\to\infty}$ versus the PRTW $\frac{P_T}{P_W}$. $E=2*10^4 J$, $P_W=1$ $W$, $\lambda=0.01$, $\alpha=3$, $\gamma=20$, $R=3$, $q\in\{0.2,0.6,1\}$. (a) $\xi_q^{*,\bar{A}_p\to\infty}$ versus $\frac{P_T}{P_W}$. (b) $M_q^{*,\bar{A}_p\to\infty}$ versus $\frac{P_T}{P_W}$.

arrival rate $\xi$ is set to be (21), shown at the bottom of the page.

Fig. 5 illustrates how the optimal packet arrival rate $\xi_q^{*,\bar{A}_p\to\infty}$ and the corresponding maximum lifetime throughput $M_q^{*,\bar{A}_p\to\infty}$ vary with the PRTW $\frac{P_T}{P_W}$ under different values of the channel access probability $q$. Similar to Fig. 2, we can see that both $\xi_q^{*,\bar{A}_p\to\infty}$ and $M_q^{*,\bar{A}_p\to\infty}$ decrease with $\frac{P_T}{P_W}$, especially when $q$ is large. Intuitively, when the channel access probability $q$ is small, i.e., $q=0.2$, the network interference is limited and the packet arrival rate $\xi$ can be set as one in the range of $\frac{P_T}{P_W}\in[1,10]$. In contrast, when channel access probability $q$ is large, i.e., $q=0.6$ and $q=1$, the network interference can be severe. In order to maintain a high probability of successful transmission and reduce the energy consumption, the optimal packet arrival rate $\xi_q^{*,\bar{A}_p\to\infty}<1$ when $\frac{P_T}{P_W}$ is relatively small, and decreases with the increase of $\frac{P_T}{P_W}$.

Moreover, from Fig. 5b, we observe that $\frac{P_T}{P_W}$ is small, a large channel access probability always leads to a better $M_q^{*,\bar{A}_p\to\infty}$. When $\frac{P_T}{P_W}$ increases, it is interesting to see that $M_q^{*,\bar{A}_p\to\infty}$ is not sensitive to the packet arrival rate $\xi$ and becomes solely dependent on $\frac{P_T}{P_W}$. In this case, as shown in Fig. 5a, the packet arrival rate is low, with which the buffer is often empty and has no new update. Thus, the variation of channel access probability has limited effect on the lifetime throughput performance.

## B. Age-Energy Optimization Tradeoff

Recall that, given the channel access probability, the packet arrival rate can be tuned to optimize the peak AoI performance [29], i.e., $\xi_{q,\text{AoI}}^*=\arg\min_\xi A_p$. Since the optimal packet arrival rate for lifetime throughput optimization $\xi_q^{*,\bar{A}_p\to\infty}$ decreases with $\frac{P_T}{P_W}$, as shown in Fig. 5a, we can have the following relationship between $\xi_q^{*,\bar{A}_p\to\infty}$ and $\xi_{q,\text{AoI}}^*$.

*Corollary 2:* The optimal packet arrival rate for peak AoI performance optimization $\xi_{q,\text{AoI}}^*$ and the optimal packet arrival rate for lifetime throughput optimization $\xi_q^{*,\bar{A}_p\to\infty}$ satisfy

$$\begin{cases}\xi_q^{*,\bar{A}_p\to\infty}\le\xi_{q,\text{AoI}}^*, & \text{if } \frac{P_T}{P_W}\ge\frac{1+q}{q},\\ \xi_q^{*,\bar{A}_p\to\infty}\ge\xi_{q,\text{AoI}}^*, & \text{if } \frac{P_T}{P_W}\le\frac{1+q}{q}.\end{cases} \tag{22}$$

*Proof:* See Lemma 3 in Appendix C. ■

Due to distinct optimal packet arrival rates, there exists a trade-off between the lifetime throughput optimization and

$$M_q^{*,\bar{A}_p\to\infty}=\begin{cases}\dfrac{E\exp\left\{-\dfrac{2}{1+\sqrt{1+\frac{4}{\lambda cR^2}\left(\frac{P_T}{P_W}-1\right)}}-\theta R^\alpha\gamma^{-1}\right\}}{P_W\left(\frac{1}{2}\lambda cR^2\left(1+\sqrt{1+\frac{4}{\lambda cR^2}\left(\frac{P_T}{P_W}-1\right)}\right)-1\right)+P_T}, & \text{if } \lambda cR^2>\dfrac{1}{\left(\frac{P_T}{P_W}-1\right)q^2+q},\\ \dfrac{Eq\exp\left\{-\lambda cR^2q-\theta R^\alpha\gamma^{-1}\right\}}{P_W(1-q)+P_Tq}, & \text{otherwise}.\end{cases} \tag{20}$$

$$\xi_q^{*,\bar{A}_p\to\infty}=\begin{cases}\dfrac{2q\exp\left\{-\dfrac{2}{1+\sqrt{1+\frac{4}{\lambda cR^2}\left(\frac{P_T}{P_W}-1\right)}}-\theta R^\alpha\gamma^{-1}\right\}}{\lambda cR^2q\left(1+\sqrt{1+\frac{4}{\lambda cR^2}\left(\frac{P_T}{P_W}-1\right)}\right)+2q\exp\left\{-\dfrac{2}{1+\sqrt{1+\frac{4}{\lambda cR^2}\left(\frac{P_T}{P_W}-1\right)}}-\theta R^\alpha\gamma^{-1}\right\}-2}, & \text{if } \lambda cR^2>\dfrac{1}{\left(\frac{P_T}{P_W}-1\right)q^2+q},\\ 1, & \text{otherwise}.\end{cases} \tag{21}$$

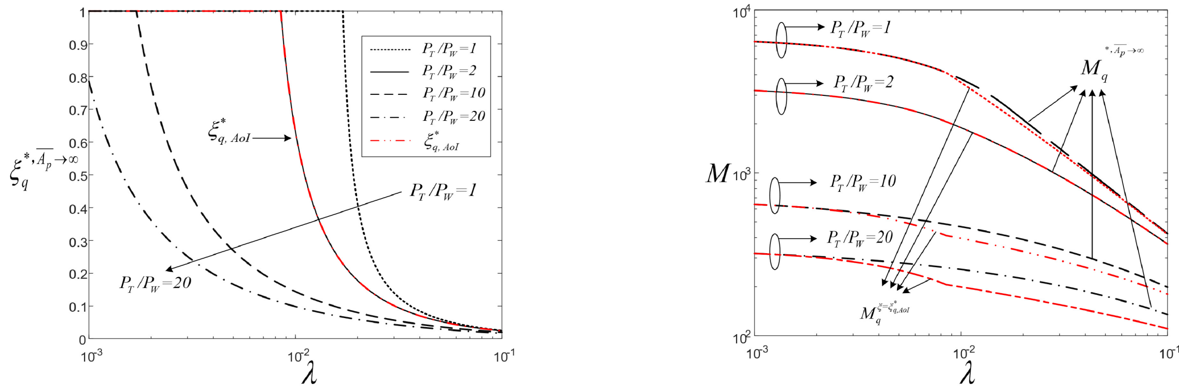

(a) (b)

Fig. 6. Optimal packet arrival rate $\xi_q^{*,\bar{A}_p\to\infty}$ and the corresponding maximum lifetime throughput $M_q^{*,\bar{A}_p\to\infty}$, $M_q^{\xi=\xi^*_{q,\mathrm{AoI}}}$ versus the node density $\lambda$. $E = 2*10^4 J$, $P_W = 1\ W$, $\lambda = 0.01$, $\alpha = 3$, $\gamma = 20$, $R = 3$, $q = 1$, $\frac{P_T}{P_W} \in \{2, 10, 20\}$. (a) $\xi_q^{*,\bar{A}_p\to\infty}$ versus $\lambda$. (b) $M_q^{*,\bar{A}_p\to\infty}$, $M_q^{\xi=\xi^*_{q,\mathrm{AoI}}}$ versus $\lambda$.

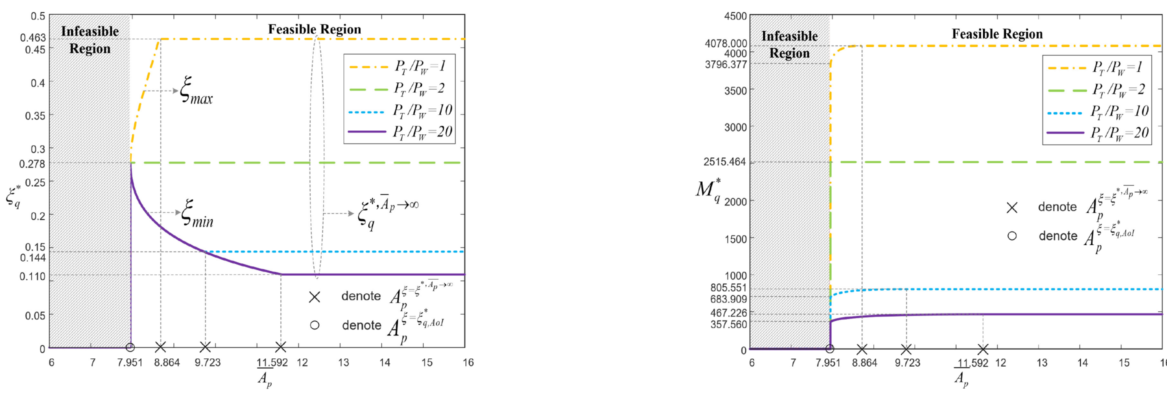

(a) (b)

Fig. 7. Optimal packet arrival rate $\xi_q^*$ and the corresponding lifetime throughput $M_q^*$ versus the AoI constraint $\bar{A}_p$. $E = 2*10^4 J$, $P_W = 1\ W$, $\lambda = 0.05$, $\alpha = 3$, $\gamma = 20$, $R = 2$, $q = 1$, $\frac{P_T}{P_W} \in \{1, 2, 10, 20\}$. $R = 2$. (a) $\xi_q^*$ versus $\bar{A}_p$ (c) $M_q^*$ versus $\bar{A}_p$.

the peak AoI optimization. Fig. 6 illustrates how the maximum lifetime throughput $M_q^{*,\bar{A}_p\to\infty}$ varies the node density $\lambda$ under different values of the PRTW $\frac{P_T}{P_W}$. The lifetime throughput $M_q^{\xi=\xi^*_{q,\mathrm{AoI}}}$ when optimal peak AoI is achieved has also been highlighted in red in the figure. We can see that the lifetime throughput performance is sacrificed with $\xi = \xi^*_{q,\mathrm{AoI}}$. The performance loss becomes significant when $\frac{P_T}{P_W}$ or $\lambda$ is large. The observation indicates that if the system considers the peak AoI performance guarantee, then the lifetime throughput may be reduced. Accordingly, we look at the lifetime throughput optimization with finite peak AoI constraints in the next part.

### C. Peak-AoI-Constrained Lifetime Throughput Optimization

With a finite peak AoI constraint $\bar{A}_p < \infty$, Fig. 7 presents the optimal packet arrival rate and the corresponding maximum lifetime throughput. We can see from Fig. 7 that the network falls into the infeasible region if $\bar{A}_p$ is too small, i.e., $\bar{A}_p < A_p^{\xi=\xi^*_{q,\mathrm{AoI}}} = 7.951$; Otherwise, the network is in the feasible region, in which case the optimal packet arrival rate crucially related on $\frac{P_T}{P_W}$. As Corollary 2 indicates, with $\frac{P_T}{P_W} = \frac{1+q}{q}$, the peak AoI and lifetime throughput can be optimized simultaneously.

As shown in Fig. 7a, the feasible region of the packet arrival rate is further segmented into two parts, i.e., (1) $\xi_q^* = \xi_{\max}$ for $\frac{P_T}{P_W} < \frac{1+q}{q}$ or $\xi_q^* = \xi_{\min}$ for $\frac{P_T}{P_W} > \frac{1+q}{q}$ when $A_p^{\xi=\xi^*_{q,\mathrm{AoI}}} \leq \bar{A}_p < A_p^{\xi=\xi_q^{*,\bar{A}_p\to\infty}}$; (2) $\xi_q^* = \xi_q^{*,\bar{A}_p\to\infty}$ When $\bar{A}_p \geq A_p^{\xi=\xi_q^{*,\bar{A}_p\to\infty}}$. In case 1, when the $\frac{P_T}{P_W} < \frac{1+q}{q}$, $\xi_q^* = \xi_{\max}$, the optimal packet arrival rate $\xi_q^*$ increases as $\bar{A}_p$ increases. When $\frac{P_T}{P_W} < \frac{1+q}{q}$, $\xi_q^* = \xi_{\min}$, the optimal packet arrival rate $\xi_q^*$ decreases as $\bar{A}_p$ increases. When the AoI constraint further relaxes, it would not affect the optimal parameter selection, where $\xi_q^*$ is solely determined by $\frac{P_T}{P_W}$. Similar observations can be obtained in Fig. 6b.

## V. Joint Optimization

So far, we have characterized the optimal tuning of the channel access probability $q$ given the packet arrival rate $\xi$, and the optimal tuning of packet arrival rate $\xi$ given the channel access probability $q$. This section will further investigate how to jointly tune the channel access probability $q$ and the packet arrival rate $\xi$ to optimize the lifetime throughput performance while satisfy the AoI constraint.

### A. Lifetime Throughput Optimization Without Constraint

Let us first examine the case when $\bar{A}_p \to \infty$. Without peak AoI constraint, the maximum lifetime throughput $M^{*,\bar{A}_p\to\infty}$ is given by

$$M^{*,\bar{A}_p\to\infty} = \begin{cases} \dfrac{\frac{E}{P_W}\exp\left\{-\frac{2}{1+\sqrt{1+\frac{4}{\lambda cR^2}\left(\frac{P_T}{P_W}-1\right)}}-\theta R^{\alpha}\gamma^{-1}\right\}}{\frac{\lambda cR^2}{2}\left(1+\sqrt{1+\frac{4}{\lambda cR^2}\left(\frac{P_T}{P_W}-1\right)}\right)+\left(\frac{P_T}{P_W}-1\right)}, & \text{if } \lambda cR^2 > \frac{P_W}{P_T}, \\ \frac{E}{P_T}\exp\left\{-\lambda cR^2-\theta R^b\gamma^{-1}\right\}, & \text{otherwise}. \end{cases} \tag{29}$$

which is achieved if and only if $(\xi^{*,\bar{A}_p\to\infty}, q^{*,\bar{A}_p\to\infty})$ satisfy

$$\left(\xi^{*,\bar{A}_p\to\infty}, q^{*,\bar{A}_p\to\infty}\right) = \begin{cases} (\xi_1, q_1), & \lambda cR^2 > \frac{P_W}{P_T}, \\ (1,\ 1), & \text{otherwise}. \end{cases} \tag{30}$$

where $(\xi_1, q_1)$ satisfies equation (24), shown at the bottom of the page. Fig. 8 illustrates how the lifetime throughput $M$ varies with the channel access probability $q$ and the packet arrival rate $\xi$. The optimal lifetime throughput $M^{*,\bar{A}_p\to\infty}$ is also identified with red marks or lines in these figures. In Fig. 8a, when $\lambda cR^2 = 0.5893 < \frac{P_W}{P_T} = 1$, $M$ can be optimized at the point $(\xi^* = 1, q^* = 1)$, which indicates that when the energy consumption for transmission is small, the system

---

*Theorem 3:* With $A_p \le \bar{A}_p$, the maximum lifetime throughput $M^*$ is achieved when

$$(\xi^*, q^*) = \begin{cases} (1,1), & \text{if } \lambda cR^2 < \frac{P_W}{P_T} \text{ and } \bar{A}_p > A_{p,\min}^{M=M^*}, \\ (\xi_2, q_2), & \text{if } \lambda cR^2 < \frac{P_W}{P_T} \text{ and } \lambda cR^2 > \frac{1}{2} \text{ and } A_p^{\xi=\xi^*_{\mathrm{AoI}}, q=q^*_{\mathrm{AoI}}} < \bar{A}_p < A_{p,\min}^{M=M^*}, \\ \text{or} & \text{if } \lambda cR^2 > \frac{P_W}{P_T} \text{ and } A_p^{\xi=\xi^*_{\mathrm{AoI}}, q=q^*_{\mathrm{AoI}}} < \bar{A}_p < A_{p,\min}^{M=M^*}, \\ (\xi_1, q_1), & \text{if } \lambda cR^2 > \frac{P_W}{P_T} \text{ and } \bar{A}_p > A_{p,\min}^{M=M^*}, \\ \text{no solution}, & \text{otherwise}. \end{cases} \tag{23}$$

where $(\xi_1, q_1)$ satisfies

$$q_1 = \frac{2}{\lambda cR^2\left(1+\sqrt{1+\frac{4}{\lambda cR^2}\left(\frac{P_T}{P_W}-1\right)}\right) - 2\exp\left\{-\frac{2}{1+\sqrt{1+\frac{4}{\lambda cR^2}\left(\frac{P_T}{P_W}-1\right)}} - \theta R^b\gamma^{-1}\right\}\left(\frac{1-\xi_1}{\xi_1}\right)}, \tag{24}$$

and $(\xi_2, q_2)$ can be obtained from the following equation

$$\underset{\left\{(\xi,q)\mid\frac{1}{\xi}+\frac{2}{qp}-1=\bar{A}_p\right\}}{\arg}\ \max\ \frac{E\xi qp}{P_W(1-q)\xi + P_I qp(1-\xi) + P_T q\xi}. \tag{25}$$

In (23), $A_{p,\min}^{M=M^*}$ is the lower bound of peak AoI in (24) when $\lambda cR^2 > \frac{P_W}{P_T}$, which is given by

$$A_{p,\min}^{M=M^*} = \left(\frac{1}{2}\lambda cR^2\left(1+\sqrt{1+\frac{4}{\lambda cR^2}\left(\frac{P_T}{P_W}-1\right)}\right)+1\right)\left(\exp\left\{\frac{2}{1+\sqrt{1+\frac{4}{\lambda cR^2}\left(\frac{P_T}{P_W}-1\right)}}+\theta R^{\alpha}\gamma^{-1}\right\}\right). \tag{26}$$

The upper bound of peak AoI $A_{p,\max}^{M=M^*}$ in (24) when $\lambda cR^2 > \frac{P_W}{P_T}$ is given by

$$A_{p,\max}^{M=M^*} = \left(\lambda cR^2\left(1+\sqrt{1+\frac{4}{\lambda cR^2}\left(\frac{P_T}{P_W}-1\right)}\right)\right)\left(\exp\left\{\frac{2}{1+\sqrt{1+\frac{4}{\lambda cR^2}\left(\frac{P_T}{P_W}-1\right)}}+\theta R^{\alpha}\gamma^{-1}\right\}\right). \tag{27}$$

Specially, when $\lambda cR^2 < \frac{P_W}{P_T}$, the lifetime throughput is optimized in $(\xi^*, q^*) = (1,1)$, and $A_{p,\min}^{M=M^*} = 2\exp\left\{\lambda cR^2 + \theta R^{\alpha}\gamma^{-1}\right\}$. The optimal peak AoI is given by [29]

$$A_p^{\xi=\xi^*_{\mathrm{AoI}}, q=q^*_{\mathrm{AoI}}} = \begin{cases} \dfrac{\lambda cR^2\left(\sqrt{1+\frac{4}{\lambda cR^2}}+1\right)+2}{2\exp\left\{-\frac{2}{\sqrt{1+\frac{4}{\lambda cR^2}}+1}-\theta R^{\alpha}\gamma^{-1}\right\}}, & \text{if } \lambda cR^2 > \frac{1}{2}, \\ 2\exp\left\{\lambda cR^2+\theta R^{\alpha}\gamma^{-1}\right\}, & \text{otherwise}. \end{cases} \tag{28}$$

*Proof:* See Appendix D. ■

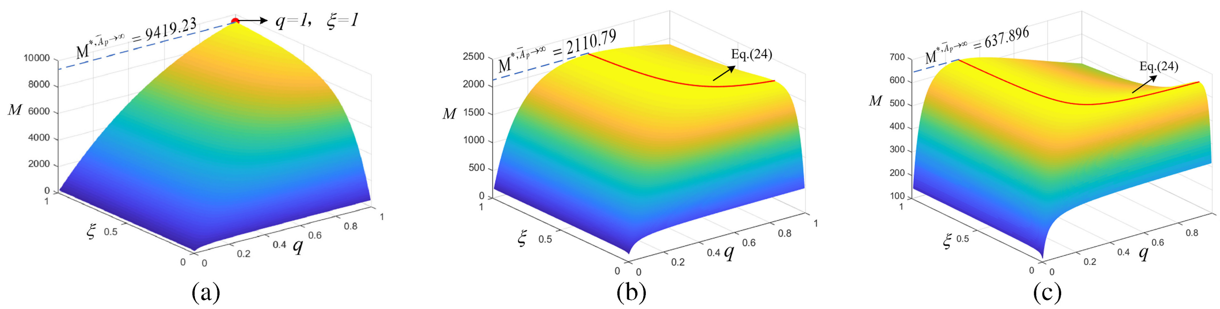


Fig. 8. The lifetime throughput $M$ versus the channel access probability $q$, packet arrival rate $\xi$. $E = 5 * 10^4 J$, $P_W = 1\ W$, $\lambda = 0.01$, $\alpha = 3$, $\gamma = 20$, $R = 3$. (a) $P_T/P_W = 1$, (b) $P_T/P_W = 5$, (c) $P_T/P_W = 20$.

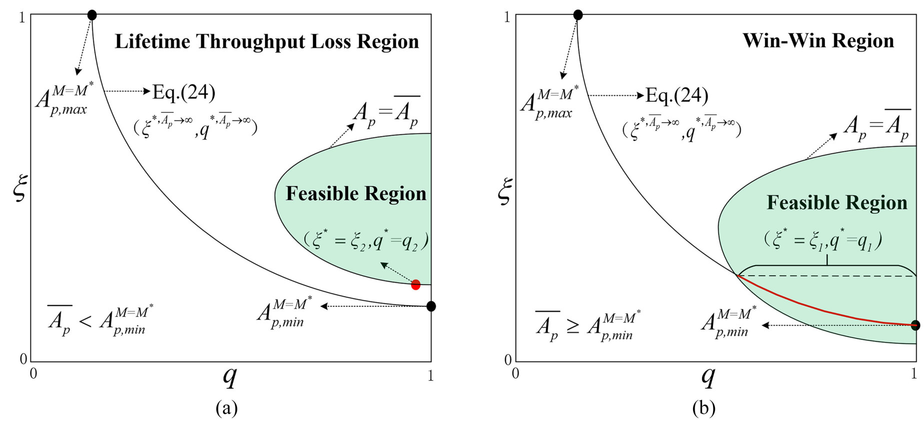


Fig. 9. Graphic illustration of feasible region when $\lambda c R^2 > \max\{\frac{P_W}{P_T}, \frac{1}{2}\}$ and $\frac{P_T}{P_W} > 2$. (a) $\bar{A}_p < A_{p,\min}^{M=M^*}$. (b) $\bar{A}_p \geq A_{p,\min}^{M=M^*}$.

should transmit packets as many as possible. In Fig. 8b and Fig. 8c, we have $\lambda c R^2 > \frac{P_W}{P_T}$, then the lifetime throughput is maximized as long as (24) holds. In this case, the maximum lifetime throughput can be achieved by either tuning the channel access probability $q$ or the packet arrival rate $\xi$, which can be regarded as adjusting the input or output of the queueing system for interference management. Moreover, without peak AoI constraint, Appendix D further shows that when $(\xi, q)$ satisfies (24), the corresponding peak AoI decreases with the channel access probability $q$ and increases with the packet arrival rate $\xi$. Based on the monotonicity of peak AoI over $q$ and $\xi$, the optimal $(\xi^*, q^*)$ for maximizing the AoI-constraint lifetime throughput can be obtained.

### B. Peak-AoI-Constrained Lifetime Throughput Optimization

With a finite peak AoI constraint $\bar{A}_p < \infty$, to understand Theorem 3, we present the graphic illustration of the feasible region[3] of $(\xi^*, q^*)$ and the curve of (24) in Fig. 9. Note that only in the feasible region can we have $(\xi^*, q^*)$; Otherwise, the joint optimization of the AoI-constrained lifetime throughput has no solution. Moreover, the pair of $(\xi, q)$ on the curve of (24) is the optimal setting for maximizing the lifetime throughput $M$ without AoI constraint. As shown in Fig. 9, the curve of (24) may or may not have the intersection with the feasible region. If the curve of (24) does not fall into the feasible region, then $(\xi_2, q_2)$ in (25), shown at the bottom of the previous page, on the boundary of the feasible region, i.e., $A_p = \bar{A}_p$, is the optimal setting, with which the maximum lifetime throughput $M^* < M^{*,\bar{A}_p \to \infty}$. We term this case as the Lifetime Throughput Loss case, as shown in Fig. 9a. On the other hand, if the curve of (24) falls into the feasible region, then all $(\xi^*, q^*)$, i.e., $(\xi_1, q_1)$, in the intersection part are optimal settings, with which the maximum lifetime throughput $M^* = M^{*,\bar{A}_p \to \infty}$. We term this case as the Win-Win case, as shown in Fig. 9b. Whether the network is in the Lifetime Throughput Loss case or in the Win-Win case closely depends on the AoI constraint.

Fig. 10 illustrates how the optimal channel access probability $q^*$, the optimal packet arrival rate $\xi^*$ and the AoI-constrained maximum lifetime throughput $M^*$ vary with the AoI constraint $\bar{A}_p$. Following the analysis in Fig. 9, the feasible region can be divided into two areas:

- *Lifetime Throughput Loss Region:* In this region, $(\xi^*, q^*) = (\xi_2, q_2)$ and the lifetime throughput is sacrificed for meeting the stringent AoI constraint. In Fig. 10b, the AoI-constrained maximum lifetime throughput $M = M^*$ is presented, where we observe that even with optimal setting $(\xi^*, q^*)$, $M = M^*$ drops from 696.79 packets to 613.98 packets, i.e., 11.9% performance loss, if the AoI constraint $\bar{A}_p$ becomes stringent. Moreover, we can also see that when the condition that $A_{p,\min}^{M=M^*} = A_p^{\xi=\xi^*_{\mathrm{AoI}}, q=q^*_{\mathrm{AoI}}}$ is satisfied, i.e., $\lambda c R^2 < \min\{\frac{P_W}{P_T}, \frac{1}{2}\}$ or $\frac{P_T}{P_W} = 2$, the peak AoI and

[3]Note that the feasibility analysis can provide important guidance on practical system design. For instance, given the peak AoI constraint, the upper-bound of the node deploy density $\lambda_{\max}$ can be obtained. Accordingly, upon the network initialization, the system should properly control the node deploy density $\lambda$ such that $\lambda < \lambda_{\max}$; Otherwise, the age constraint cannot be guaranteed regardless of $q$ and $\xi$.

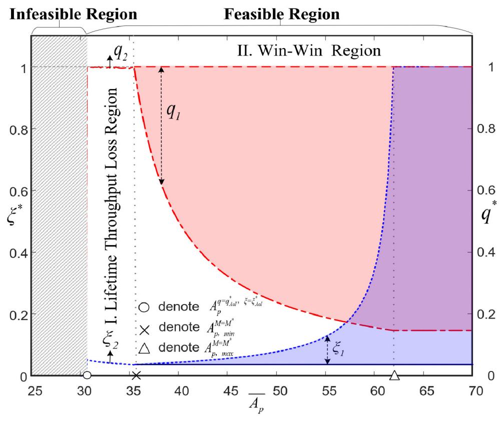


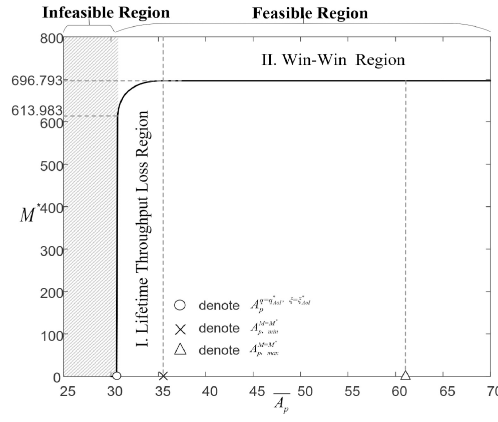


Fig. 10. Optimal channel access probability $q^*$ and packet arrival rate $\xi^*$ and the corresponding maximum lifetime throughput $M^*$ versus the peak AoI constraint $\bar{A}_p$. $E = 5 * 10^4 J$, $P_W = 1$ $W$, $\lambda = 0.05$, $\alpha = 3$, $\gamma = 20$, $R = 3$, $\frac{P_T}{P_W} = 10$. $R = 3$. (a) $q^*$, $\xi^*$ versus $\bar{A}_p$ (c) $M^*$ versus $\bar{A}_p$.

the lifetime throughput can be optimized simultaneously, and the lifetime throughput loss region not exist. The former indicates that the lifetime throughput and peak AoI can be optimized simultaneously when the network interference is not significant. Both of them benefit from the highest frequency updates, i.e., $(\xi^* = 1, q^* = 1)$. The latter shows that when the interference is prominent, the lifetime throughput and peak AoI can be optimized simultaneously only when PRTW equals two.

- *Win-Win Region:* In this region, $(\xi^*, q^*) = (\xi_1, q_1)$ in (24). The maximum lifetime throughput $M^* = M^{*,\bar{A}_p \to \infty}$. In particular, we observe that when $\bar{A}_p > A_{p,\max}^{M=M^*}$, the peak AoI constraint does not influence the optimal setting any more.

So far, by addressing the age-constrained lifetime throughput maximization problem, we have evaluated the age-energy tradeoff in slotted Aloha-based Poisson bipolar networks. The analysis can be extended to a variety of D2D communication systems by relaxing a few key assumptions:

*1) Packet arrival pattern:* In IoT applications, the packet arrival pattern can be categorized into two modes: event-triggered mode and time-triggered mode. In the event-triggered mode, IoT devices deliver packets once the targeted event is detected. As the targeted events may happen randomly over time, the packet arrival process is random as well. In the time-triggered mode, IoT devices perform the sampling operation periodically such that packets arrive with fixed time interval. In this paper, we consider the event-triggered mode by taking the example of Bernoulli arrivals. The analysis can be extended to the time-triggered mode, where the *D*/*Geo*/1/1 model can be used to characterize the queueing behavior of each transmitter.

*2) Symmetric/Non-symmetric setting:* This paper considers the symmetric setting, where all devices have the same traffic input rate and channel access probability. Yet, in practical scenarios, different IoT applications may coexist in the same network, where devices may have distinct traffic characteristics and parameter settings. The proposed analytical framework can further be extended by grouping devices with the same characteristics into one group, with parameters differing from group to group. It is conjectured that transmitters could have distinct probabilities of successful transmission for each group, which could be jointly determined by a set of non-linear equations. The corresponding computational complexity increases rapidly as the number of groups in the network grows. How to reduce the computational complexity and further optimize the age-energy tradeoff deserves future study.

*3) Rechargeable/Non-rechargeable battery:* In this paper, we assume the battery of each device cannot be replenished or recharged, such that the life of a transmitter comes to an end if its energy runs out. The analysis in this paper can be extended to the rechargeable battery case, e.g., energy harvesting powered wireless sensor networks. In this case, the behavior of the HoL packet crucially depends on the energy harvesting rate. To characterize the arrival process of data packet and that of the external power, a double-queue model can be established, which contains two queues: the data queue and the energy queue. A two-dimensional Markov process can be used to analyze the dynamics and coupling among those two queues.

## VI. Conclusion

This paper maximizes the lifetime throughput of each node in mobile random access Poisson bipolar networks with the peak AoI constraint by individually and jointly tuning the channel access probability and the packet arrival rate. The effect of system parameters, such as node deployment density, the PRTW and the peak AoI threshold, on the maximum lifetime throughput and the corresponding optimal transmission parameters is investigated.

The analysis sheds essential light on energy efficiency-oriented design for large-scale freshness-aware IoT networks. Specifically, it indicates that when the network interference is not significant, the lifetime throughput and peak AoI both benefit from frequent updates and transmissions. When the network interference is severe, an age-energy tradeoff may exist, and the performance gap between the maximum lifetime throughput without AoI constraint and AoI-optimal lifetime throughput enlarges if the PRTW is too large. Moreover, it is found that the peak AoI constraint would affect the lifetime throughput performance only if the constraint is stringent. To achieve the AoI-constrained maximum lifetime throughput, the channel access probability and the packet arrival rate should be optimally tuned according to the analysis.

## APPENDIX A
## DERIVATION OF (4)

According to the total lifetime of each node, we have

$$T = T_S + T_F + T_W + T_I, \tag{31}$$

and according to the total energy constraint of each node and $P_I = P_W$, we have

$$\begin{aligned} E &= P_W T_W + P_I T_I + P_T(T_S + T_F) \\ &= P_W(T_W + T_I) + P_T(T_S + T_F), \end{aligned} \tag{32}$$

In each transmission attempt, with probability $p$, the transmitter spends one time slot in successful transmissions; otherwise, with probability $1 - p$, it spends one time slot in failure. We then have

$$\frac{T_S}{T_F} = \frac{p}{1-p}. \tag{33}$$

Recall that each transmitter accesses the channel with probability $q$ in each time slot; otherwise, it stays in the waiting state. Thus, we have

$$\frac{T_W}{T_S + T_F} = \frac{1-q}{q}. \tag{34}$$

Since the mean service rate of each queue is given by $qp$, we have

$$\frac{T_S}{T_W + T_S + T_F} = qp. \tag{35}$$

Let $\rho$ denote the non-empty probability of each transmitter's queue which has been derived in [29] as $\rho = \frac{\xi}{\xi + qp - \xi qp}$. By definition, we have

$$\frac{T_W + T_S + T_F}{T_I} = \frac{\rho}{1-\rho}. \tag{36}$$

Since one packet lasts for one time slot, the lifetime throughput $M$ equals that the product of the throughput and its lifetime length $T$. Then, (4) can be obtained by combining (31)-(36).

## APPENDIX B
## PROOF OF THEOREM 1

First, we derive the unconstrained maximum lifetime throughput $M_\xi^{*,\bar{A}_p\to\infty}$ and the corresponding optimal channel access probability $q_\xi^{*,\bar{A}_p\to\infty}$. According to (2) and (4), we have

$$\frac{\partial M}{\partial q} = \frac{\frac{E\lambda c R^2 \left(\frac{\xi}{q}\right)^2 p}{\lambda c R^2 p\xi(1-\xi) - \left(\frac{\xi}{q} + p(1-\xi)\right)^2}\left(P_W(1-q)q\xi^2 + P_T q^2\xi^2\right) + P_W\xi^2 p}{(P_W(1-q)\xi + P_I qp(1-\xi) + P_T q\xi)^2}. \tag{37}$$

We then have $\lim_{q\to 0}\frac{\partial M}{\partial q} = E\frac{P_W p}{(P_W + P_T)^2} > 0$, and

$$\lim_{q\to 1}\frac{\partial M}{\partial q} = E\frac{\frac{\lambda c R^2\xi^2 p_*}{\lambda c R^2 p_*\xi(1-\xi) - [\xi + p_*(1-\xi)]^2}P_T\xi^2 + P_W\xi^2 p_*}{\left(P_I p_*(1-\xi) + P_T\xi\right)^2}, \tag{38}$$

where $p_*$ is the non-zero root of (9), shown at the bottom of p. 9. Substituting $P_I = P_W$ into (38), we have $\lim\limits_{q\to 1}\frac{\partial M}{\partial q} < 0$ when $\lambda c R^2 > \frac{[\xi + p_*(1-\xi)]^2}{\xi^2\frac{P_T}{P_W} + p_*\xi(1-\xi)}$. The lifetime throughput can then be optimized when $q \in (0, 1)$. By combining $\frac{\partial M}{\partial q} = 0$ and (2), the optimal channel access probability can be obtained as (13), and the corresponding probability of successful transmission $p$ can be expressed as

$$p = \exp\left\{-\frac{2}{1 + \sqrt{1 + \frac{4}{\lambda c R^2}\left(\frac{P_T}{P_W} - 1\right)}} - \theta R^\alpha \gamma^{-1}\right\}. \tag{39}$$

The optimal lifetime throughput can be obtained by substituting (13) and (39) into (4). When $\lambda c R^2 \le \frac{[\xi + p_*(1-\xi)]^2}{\xi^2\frac{P_T}{P_W} + p_*\xi(1-\xi)}$, on the other hand, the optimal channel access probability is given by $q = 1$, and the corresponding lifetime throughput can be obtained by combining $q = 1$ and (4).

With the constraint $A_p \le \bar{A}_p$, Lemma 1 shows the feasible region of channel access probability.

*Lemma 1:* When $A_p \le \bar{A}_p$ is required, the feasible region of channel access probability $q$ is given by

$$\mathbf{q} = \begin{cases} [q_{\min}, q_{\max}] & \text{if } A_p^{q=q^*_{\xi,\mathrm{AoI}}} \le \bar{A}_p < A_p^{q=1} \\ [q_{\min}, 1] & \text{if } \bar{A}_p \ge A_p^{q=1} \\ \varnothing & \text{if } \bar{A}_p < A_p^{q=q^*_{\xi,\mathrm{AoI}}} \end{cases} \tag{40}$$

where $q_{\min}$ has been given in (8), shown at the bottom of p. 5, and $q_{\max}$ can be expressed as $q_{\max} = \frac{\mathbb{W}_{-1}\left(-\frac{2\lambda c R^2\xi\exp\{\theta R^\alpha\gamma^{-1}\}}{2(1-\xi) + \xi(\bar{A}_p - \frac{1}{\xi} + 1)}\right)}{-\frac{\lambda c R^2\xi(\bar{A}_p - \frac{1}{\xi} + 1)}{2(1-\xi) + \xi(\bar{A}_p - \frac{1}{\xi} + 1)}}$. The expression of $A_p^{q=q^*_{\xi,\mathrm{AoI}}}$ is given by (10), shown at the bottom of p. 5, and $A_p^{q=1} = \frac{1}{\xi} + \frac{2}{p_*} - 1$.

*Proof:* Due to lack of space, we sketch the outline. The feasible region analysis in Lemma 1 is based on the fact that $A_p$ in terms of $q$ has only one peak point at most [29]. Then $q_{\min}$ and $q_{\max}$ can be derived from $A_p = \bar{A}_p$. ■

Lemma 2 in the following simplifies the analysis of the constraint optimization problem.

*Lemma 2:* With the same system parameter setting, $q_\xi^{*,\bar{A}_p\to\infty} \le q^*_{\xi,\mathrm{AoI}}$ always holds.

*Proof:* The optimal channel access probability for lifetime throughput maximization can be expressed as (13). The optimal channel access probability for peak AoI optimization has been derived in [29], which is given by

$$q^*_{\xi,\mathrm{AoI}} = \begin{cases} \frac{1}{\lambda c R^2 - \frac{1-\xi}{\xi}\exp\{-\theta R^\alpha\gamma^{-1} - 1\}} & \text{if } \lambda c R^2 > 1 + \frac{p_*(1-\xi)}{\xi} \\ 1 & \text{otherwise}. \end{cases} \tag{41}$$

With $P_T \ge P_W$, we have

$$\frac{[\xi + p_*(1-\xi)]^2}{\xi^2\frac{P_T}{P_W} + p_*\xi(1-\xi)} < \frac{[\xi + p_*(1-\xi)]^2}{\xi^2 + p_*\xi(1-\xi)} = 1 + \frac{p_*(1-\xi)}{\xi}, \tag{42}$$

which indicates that when $q^*_{\xi,\mathrm{AoI}} < 1$, we have $q_\xi^{*,\bar{A}_p\to\infty} < 1$ as well.

Let us further prove $q_\xi^{*,\bar{A}_p\to\infty} \le q_{\xi,\mathrm{AoI}}^*$ by considering the following two cases:

1) $\lambda c R^2 > \frac{[\xi+p_*(1-\xi)]^2}{\xi^2+p_*\xi(1-\xi)}$: based on (13), (41) and (42), we have $q_\xi^{*,\bar{A}_p\to\infty} < 1$ and $q_{\xi,\mathrm{AoI}}^* < 1$. Denote $t = \frac{1+\sqrt{1+\frac{4}{\lambda c R^2}(\frac{P_T}{P_W}-1)}}{2}$, $A = \lambda c R^2$ and $B = e^{-\theta R^\alpha \gamma^{-1}\frac{1-\xi}{\xi}}$. Then, we have

$$\frac{q_{\xi,\mathrm{AoI}}^*}{q_\xi^{*,\bar{A}_p\to\infty}} = \frac{At - Be^{-\frac{1}{t}}}{A - Be^{-1}} \quad t \in [1,+\infty). \tag{43}$$

Let $f(t) = At - Be^{-\frac{1}{t}}$. The derivative $f'(t)$ satisfies

$$f'(t) = A - \tfrac{B}{t^2}e^{-\frac{1}{t}} > f'(1) = A - Be^{-1} > 0. \tag{44}$$

$f(t)$ thus increases monotonically when $t \in [1,+\infty)$, we then have $\frac{q_{\xi,\mathrm{AoI}}^*}{q_\xi^{*,\bar{A}_p\to\infty}} \ge 1$.

2) $\lambda c R^2 \le \frac{[\xi+p_*(1-\xi)]^2}{\xi^2+p_*\xi(1-\xi)}$: we have that $q_{\xi,\mathrm{AoI}}^* = 1$, and $q_\xi^{*,\bar{A}_p\to\infty} \le 1$, according to (13), (41) and (42). Thus, we have $\frac{q_{\xi,\mathrm{AoI}}^*}{q_\xi^{*,\bar{A}_p\to\infty}} \ge 1$. ∎

From Lemma 2, we obtain that $q_{\min} \ge q_\xi^{*,\bar{A}_p\to\infty}$, which means the optimal channel access probability is only determined by the the larger one between $q_{\min}$ and $q_\xi^{*,\bar{A}_p\to\infty}$, i.e., we have $q_\xi^* = \max\{q_{\min}, q_\xi^{*,\bar{A}_p\to\infty}\}$. Theorem 1 can be obtained by combining Lemma 1, $q_\xi^* = \max\{q_{\min}, q_\xi^{*,\bar{A}_p\to\infty}\}$ and $P_W = P_I$.

## Appendix C
## Proof of Theorem 2

First, we derive the unconstrained maximum lifetime throughput $M_q^{*,A_p\to\infty}$ and the corresponding optimal channel access probability $\xi_q^{*,\bar{A}_p\to\infty}$. According to (2) and (4), we have

$$\frac{\partial M}{\partial \xi} = E\frac{\frac{\lambda c R^2 p^2 \xi^2}{\lambda c R^2 p\xi(1-\xi)-\left(\frac{\xi}{q}+p(1-\xi)\right)^2}\left(P_W q(1-q)+P_T q^2\right)+P_I q^2 p^2}{[P_W(1-q)\xi+P_I qp(1-\xi)+P_T q\xi]^2}. \tag{45}$$

We then have $\lim_{\xi\to 0}\frac{\partial M}{\partial \xi} = \frac{E}{P_I} > 0$, and

$$\lim_{\xi\to 1}\frac{\partial M}{\partial \xi} = E\frac{-\lambda c R^2 p^2 q^2\left(P_W q(1-q)+P_T q^2\right)+P_I q^2 p^2}{[P_W(1-q)+P_T q]^2}, \tag{46}$$

By substituting $P_I = P_W$ into (46), we have $\lim_{\xi\to 1}\frac{\partial M}{\partial \xi} < 0$, when $\lambda c R^2 > \frac{1}{(\frac{P_T}{P_W}-1)q^2+q}$. The lifetime throughput $M$ can then be optimized when $\xi \in (0,1)$.

When $\lambda c R^2 > \frac{1}{(\frac{P_T}{P_W}-1)q^2+q}$, by combining $\frac{\partial M}{\partial \xi} = 0$ and (2), the optimal packet arrival rate in (21) can be obtained, and the probability of successful transmission $p$ as same as (39). The optimal lifetime throughput can then be obtained by combining (4), (21) and (39).

When $\lambda c R^2 \le \frac{1}{(\frac{P_T}{P_W}-1)q^2+q}$, the optimal packet arrival rate is given by $\xi = 1$, and the corresponding optimal lifetime throughput $M$ can be obtained by combining $\xi = 1$ and (4).

In the following, Let us prove the Corollary 2 to simplify the analysis of the constraint optimization problem. Consider that, when $\lambda c R^2 > \max\{\frac{1}{2q}, \frac{1}{(\frac{P_T}{P_W}-1)q^2+q}\}$, the optimal packet arrival rate $\xi < 1$ in the peak AoI optimization [29] and the lifetime throughput optimization can both be written as

$$\xi(t) = \frac{2qe^{-\frac{2}{t}}e^{-\theta R^b \gamma^{-1}}}{\lambda c R^2 qt + 2qe^{-\frac{2}{t}}e^{-\theta R^b\gamma^{-1}} - 2}. \tag{47}$$

When $t = \sqrt{1+\frac{4}{\lambda c R^2 q}}+1$, $\xi(t)$ equals the optimal packet arrival rate in optimal tuning the peak AoI $\xi_{q,\mathrm{AoI}}^*$. When $t = \sqrt{1+\frac{4}{\lambda c R^2}(\frac{P_T}{P_W}-1)}+1$, $\xi(t)$ equals the optimal packet arrival rate in optimal tuning the lifetime throughput $\xi_q^{*,\bar{A}_p\to\infty}$. Furthermore, when $t > 2$, $\xi(t)$ decreases as the $t$ increases. Thus, when $\frac{4}{\lambda c R^2}(\frac{P_T}{P_W}-1) \ge \frac{4}{\lambda c R^2 q}$, i.e., $q \ge \frac{1}{\frac{P_T}{P_W}-1}$, we have $\xi_q^{*,\bar{A}_p\to\infty} \le \xi_{q,\mathrm{AoI}}^*$; otherwise, we have $\xi_{q,\mathrm{AoI}}^* \le \xi_q^{*,\bar{A}_p\to\infty}$. Then, when $q \ge \frac{1}{\frac{P_T}{P_W}-1}$ can be satisfied, we have

$$\tfrac{1}{2q} \le \frac{1}{\left(\frac{P_T}{P_W}-1\right)q^2+q}. \tag{48}$$

The two sides of (48) are also the boundaries of the optimal packet arrival rate $\xi = 1$ and $\xi < 1$, which indicates the quantitative relationship still holds when $\lambda c R^2 \le \max\{\frac{1}{2q}, \frac{1}{(\frac{P_T}{P_W}-1)q^2+q}\}$.

Lemma 3 shows the results of the optimal packet arrival rate with AoI constraint.

*Lemma 3:* The optimal packet arrival rate that maximizes the lifetime throughput can be expressed as

$$\xi_q^* = \begin{cases} \max\left\{\xi_{\min}, \xi_q^{*,\bar{A}_p\to\infty}\right\}, & \text{if } \frac{P_T}{P_W} \ge \frac{1}{q}+1, \\ \min\left\{\xi_{\max}, \xi_q^{*,\bar{A}_p\to\infty}\right\}, & \text{if } \frac{P_T}{P_W} \le \frac{1}{q}+1, \end{cases} \tag{49}$$

where $\xi_{\min}$ and $\xi_{\max}$ are obtained from $A_p = \bar{A}_p$. Specifically,

1) if $A_p = \bar{A}_p$ does not have any root, then the optimization problem has no feasible solutions;

2) if $A_p = \bar{A}_p$ has one root, then the root is $\xi_{\min}$, and $\xi_{\max} = 1$;

3) if $A_p = \bar{A}_p$ has two roots, then the smaller root is $\xi_{\min}$, and the larger root is $\xi_{\max}$.

*Proof:* First, the root analysis in Lemma 3 is based on the fact that the function of $A_p$ has only one peak point at most [29] and therefore its details are omitted here. Thus, the feasible region of packet arrival rate, if exist, can be expressed as $[\xi_{\min}, \xi_{\max}]$.

Then, we prove (49). From above analysis, we obtain that the lifetime throughput $M$ with respect to the packet arrival rate $\xi$ has one peak point at most. Consider the following cases.

1) $q \geq \frac{1}{\frac{P_T}{P_W}-1}$: from Corollary 2, we have $\xi_q^{*,\bar{A}_p\to\infty} \leq \xi_{q,\text{AoI}}^*$, thus we have $\xi_{\max} \geq \xi_{q,\text{AoI}}^* \geq \xi_q^{*,\bar{A}_p\to\infty}$. Then, the lifetime throughput can be optimized in $\xi_q^* = \max\{\xi_{\min}., \xi_q^{*,\bar{A}_p\to\infty}\}$.

2) $q \leq \frac{1}{\frac{P_T}{P_W}-1}$: from Corollary 2, we have $\xi_q^{*,\bar{A}_p\to\infty} \geq \xi_{q,\text{AoI}}^*$, thus we have $\xi_{\min} \leq \xi_{q,\text{AoI}}^* \leq \xi_q^{*,\bar{A}_p\to\infty}$. Then, the lifetime throughput can be optimized in $\xi_q^* = \min\{\xi_{\max}, \xi_q^{*,\bar{A}_p\to\infty}\}$. ∎

The equation (16) can be derived by combining (2) and $A_p = \bar{A}_p$. Theorem 2 can be obtained by combining Lemma 3, (16) and $P_W = P_I$.

## Appendix D
## Proof of Theorem 3

By combining $\frac{\partial M}{\partial q} = 0$ and $\frac{\partial M}{\partial \xi} = 0$, we have

$$\lambda c R^2 \xi^2 \left(\frac{1}{q} - 1 + \frac{P_T}{P_W}\right) + \left(\lambda c R^2 p \xi (1-\xi) - \left(\frac{\xi}{q} + p(1-\xi)\right)^2\right) = 0, \tag{50}$$

where the probability of successful transmission $p$ is unrelated with $\xi$ and $q$, and given by (39). We then have

$$\lambda c R^2 = \frac{\left(\frac{1}{q} + \frac{p(1-\xi)}{\xi}\right)^2}{\left(\frac{1}{q} + \frac{p(1-\xi)}{\xi}\right) + \left(\frac{P_T}{P_W} - 1\right)} \geq \frac{P_W}{P_T}. \tag{51}$$

with the equality only holds when $(\xi, q) = (1,1)$. Therefore, we have

1) when $\lambda c R^2 < P_W/P_T$, (51) has no root, we have $\frac{\partial M}{\partial q} > 0$ and $\frac{\partial M}{\partial \xi} > 0$. The lifetime throughput $M$ is maximized at the point $(\xi, q) = (1,1)$.

2) when $\lambda c R^2 = P_W/P_T$, (51) has one root only when $(\xi, q) = (1,1)$. Therefore, the lifetime throughput $M$ is maximized at the point $(\xi, q) = (1,1)$.

3) when $\lambda c R^2 > P_W/P_T$, the lifetime throughput $M$ can be optimized at the point $(\xi, q) = (\xi_1, q_1)$, which are the roots of the (51). Eq. (24) can be obtained by combining (39) and (51).

Lemma 4 presents the monotonicity property of peak AoI with regard to channel access probability $q$ and packet arrival rate $\xi$ when the optimal lifetime throughput $M^*$ is achieved, i.e., $(\xi, q)$ satisfies (24).

*Lemma 4:* When $(\xi, q)$ satisfies (24), the peak AoI decreases with the channel access probability $q$, and increases with the packet arrival rate $\xi$. Moreover, the minimum peak AoI in (24) can be expressed as (26), shown at the bottom of p. 11, which is achieved when $q = 1$, and the maximum peak AoI in (24) can be expressed as (27), shown at the bottom of p. 11, which is achieved when $\xi = 1$.

*Proof:* When $\lambda c R^2 > P_W/P_T$, for all the $(\xi_1, q_1)$ satisfy (24), the peak AoI can be expressed as

$$A_p = 1 - \frac{1}{\xi_1} + \left(\left(\sqrt{(\lambda c R^2)^2 + 4\lambda c R^2\left(\frac{P_T}{P_W} - 1\right)} + \lambda c R^2\right)\right.$$

$$\left.\cdot \exp\left\{\frac{2}{1+\sqrt{1+\frac{4}{\lambda c R^2}\left(\frac{P_T}{P_W}-1\right)}} + \theta R^\alpha \gamma^{-1}\right\}\right). \tag{52}$$

It is easy to observe that the peak AoI increases with the packet arrival rate. Moreover, the packet arrival rate decreases as channel access probability in (24) increases. Thus, the peak AoI increases as the channel access probability decreases. From (24), we have

$$\sqrt{(\lambda c R^2)^2 + 4\lambda c R^2\left(\frac{P_T}{P_W} - 1\right)} + \lambda c R^2 - 2p\frac{1-\xi}{\xi} \geq 2. \tag{53}$$

Therefore, the tunable region of $\xi$ and $q$ can be expressed as

$$\begin{cases} \dfrac{2p}{\lambda c R^2\left(1+\sqrt{1+\frac{4}{\lambda c R^2}\left(\frac{P_T}{P_W}-1\right)}\right)+2p-2} \leq \xi \leq 1. \\ \dfrac{1}{\frac{\lambda c R^2}{2}\left(1+\sqrt{1+\frac{4}{\lambda c R^2}\left(\frac{P_T}{P_W}-1\right)}\right)} \leq q \leq 1. \end{cases} \tag{54}$$

∎

As a special case, when $\lambda c R^2 \leq P_W/P_T$, we have $(\xi^*, q^*) = (1,1)$. The corresponding peak AoI is given by $A_{p,\min}^{M=M^*} = 2\exp\{\lambda c R^2 + \theta R^\alpha \gamma^{-1}\}$.

Lemma 4 indicates the monotone characteristic of peak AoI in (24), leading to an observation that when a peak AoI constraint $\bar{A}_p$ is given, the boundary $\bar{A}_p = A_p$ of the feasible region and the curve of $(\xi^*, q^*)$ that satisfies (24) only have one intersection point at most. Then, we consider AoI-constraint energy efficiency optimization in the following cases:

1) $\lambda c R^2 < \min\{\frac{P_W}{P_T}, \frac{1}{2}\}$: if $\bar{A}_p > A_p^*$, then we have $(\xi^*, q^*) = (1,1)$.
2) $\lambda c R^2 \leq P_W/P_T$ and $\lambda c R^2 > \frac{1}{2}$: $(\xi, q) = (1,1)$ can be used to optimize lifetime throughput, and the optimal parameter to optimize peak AoI satisfy that $\xi_{\text{AoI}}^* < 1$ and $q_{\text{AoI}}^* = 1$.
   - when $A_p^{\xi=\xi_{\text{AoI}}^*, q=q_{\text{AoI}}^*} < A_{p,\min}^{M=M^*}$, the unconstrained optimal $M^{*,\bar{A}_p\to\infty}$ can not be achieved since $(\xi^{*,\bar{A}_p\to\infty}, q^{*,\bar{A}_p\to\infty}) = (1,1)$ is not in the feasible region. The constraint optimal parameters can be found in the boundary of $A_p = \bar{A}_p$. The solution can be expressed as $(\xi, q) = \arg\max_{\{(\xi,q)|\frac{1}{\xi}+\frac{2}{qp}-1=\bar{A}_p\}} M$.
   - when $\bar{A}_p \geq A_{p,\min}^{M=M^*}$, $(\xi^{*,\bar{A}_p\to\infty}, q^{*,\bar{A}_p\to\infty}) = (1,1)$ in the feasible domain. The optimal lifetime throughput $M^*$ can be achieved in $(\xi^*, q^*) = (1,1)$.
3) $\lambda c R^2 > \frac{P_W}{P_T}$: the point of $(\xi^*, q^*)$ to optimize the lifetime throughput satisfies (24). Moreover, in joint optimal tuning of peak AoI, we have $\xi_{\text{AoI}}^* \leq 1$ and $q_{\text{AoI}}^* = 1$ according to [29]. Thus,
   - when $A_p^{\xi=\xi_{\text{AoI}}^*, q=q_{\text{AoI}}^*} \leq \bar{A}_p < A_{p,\min}^{M=M^*}$, the unconstrained optimal $M^{*,\bar{A}_p\to\infty}$ can not be achieved due to the peak AoI constraint. In other words, the feasible region has no intersection point with (24). Then, the optimal parameters can be found in the boundary

of $A_p = \bar{A}_p$. The solution can be expressed as $(\xi, q) = \arg_{\{(\xi,q)|\frac{1}{\xi}+\frac{2}{qp}-1=\bar{A}_p\}} \max M$.

- when $\bar{A}_p \geq A_{p,\min}^{M=M^*}$, unconstrained optimal $M^{*,\bar{A}_p\to\infty}$ can be achieved. In this case,
  - when $\bar{A}_p < A_{p,\max}^{M=M^*}$, only part of (24) lies in the feasible region. The tunable region of the optimal parameters to achieve $M^{*,\bar{A}_p\to\infty}$ is limited when $A_{p,\min}^{M=M^*} \leq \bar{A}_p \leq A_{p,\max}^{M=M^*}$. By combining $A_p \leq \bar{A}_p$ and (24), the tunable region of $(\xi, q)$ can be expressed as

$$\begin{cases} \dfrac{2}{2p\bar{A}_p - \left(\lambda c R^2 \left(\sqrt{1+\frac{4}{\lambda c R^2}\left(\frac{P_T}{P_W}-1\right)}+1\right)\right)} \leq q \leq 1, \\ \dfrac{2p}{\lambda c R^2 \left(1+\sqrt{1+\frac{4}{\lambda c R^2}\left(\frac{P_T}{P_W}-1\right)}\right)+2p-2} \leq \xi, \\ \dfrac{p}{\left(\lambda c R^2 \left(\sqrt{1+\frac{4}{\lambda c R^2}\left(\frac{P_T}{P_W}-1\right)}+1\right)\right)-p(\bar{A}_p-1)} \geq \xi. \end{cases} \tag{55}$$

  - when $\bar{A}_p \geq A_{p,\max}^{M=M^*}$, the tunable parameter of (24) all lies in the feasible region, and the information freshness constraint is released regarding the problem (5).

## REFERENCES

[1] F. Zhao, X. Sun, W. Zhan, B. Zhou, and X. Huang, "AoI-constrained energy efficiency optimization in random-access poisson networks," in *Proc. IEEE WCNC*, Austin, TX, USA, Apr. 2022, pp. 1123–1128.

[2] A. Pantelopoulos and N. G. Bourbakis, "A survey on wearable sensor-based systems for health monitoring and prognosis," *IEEE Trans. Syst., Man, Cybern. C, Appl. Rev.*, vol. 40, no. 1, pp. 1–12, Jan. 2010.

[3] C. Guo, X. Wang, L. Liang, and G. Y. Li, "Age of information, latency, and reliability in intelligent vehicular networks," *IEEE Network*, early access, Sep. 2022.

[4] L. D. Xu, W. He, and S. Li, "Internet of Things in industries: A survey," *IEEE Trans. Ind. Informat.*, vol. 10, no. 4, pp. 2233–2243, Nov. 2014.

[5] S. B. Baker, W. Xiang, and I. Atkinson, "Internet of Things for smart healthcare: Technologies, challenges, and opportunities," *IEEE Access*, vol. 5, pp. 26521–26544, 2017.

[6] X. Sun, W. Zhan, W. Liu, Y. Li, and Q. Liu, "Sum rate and access delay optimization of short-packet al.ha," *IEEE Open J. Commun. Soc.*, vol. 3, pp. 1501–1514, 2022.

[7] "Green 5G: Building a sustainable world," Huawei Technol. Co., Ltd., Shenzhen, China, White Paper, Aug. 2020. Accessed: Mar. 16, 2022. [Online]. Available: https://www.huawei.com/en/public-policy/green-5g-building-a-sustainable-world

[8] F. Bouabdallah, C. Zidi, R. Boutaba, and A. Mehaoua, "Collision avoidance energy efficient multi-channel MAC protocol for underwater acoustic sensor networks," *IEEE Trans. Mobile Comput.*, vol. 18, no. 10, pp. 2298–2314, Oct. 2019.

[9] A. Maatouk, M. Assaad, and A. Ephremides, "Energy efficient and throughput optimal CSMA scheme," *IEEE/ACM Trans. Netw.*, vol. 27, no. 1, pp. 316–329, Feb. 2019.

[10] Y. Pang, W. Zhan, X. Sun, Z. Luo, and Y. Zhang, "Throughput-constrained energy efficiency optimization for CSMA networks," in *Proc. IEEE Globecom Commun. Conf.*, Rio de Janeiro, Brazil, Dec. 2022.

[11] G. Miao, A. Azari, and T. Hwang, "$E^2$-MAC: Energy efficient medium access for massive M2M communications," *IEEE Trans. Commun.*, vol. 64, no. 11, pp. 4720–4735, Nov. 2016.

[12] M. Koseoglu, E. Karasan, and L. Chen, "Cross-layer energy minimization for underwater aloha networks," *IEEE Syst. J.*, vol. 11, no. 2, pp. 551–561, Jun. 2017.

[13] Y. S. Soh, T. Q. S. Quek, M. Kountouris, and H. Shin, "Energy efficient heterogeneous cellular networks," *IEEE J. Sel. Areas Commun.*, vol. 31, no. 5, pp. 840–850, May 2013.

[14] F. Z. Djiroun and D. Djenouri, "MAC protocols with wake-up radio for wireless sensor networks: A review," *IEEE Commun. Surveys Tuts.*, vol. 19, no. 1, pp. 587–618, 1st Quart., 2017.

[15] F. Meshkati, H. V. Poor, S. C. Schwartz, and N. B. Mandayam, "An energy-efficient approach to power control and receiver design in wireless data networks," *IEEE Trans. Commun.*, vol. 53, no. 11, pp. 1885–1894, Nov. 2005.

[16] M. Kim, S. Shin, and J.-M. Chung, "Distributed power control for enhanced spatial reuse in CSMA/CA based wireless networks," *IEEE Trans. Wireless Commun.*, vol. 13, no. 9, pp. 5015–5027, Sep. 2014.

[17] X. Zhang and K. G. Shin, "E-MiLi: Energy-minimizing idle listening in wireless networks," *IEEE Trans. Mobile Comput.*, vol. 11, no. 9, pp. 1441–1454, Sep. 2012.

[18] A. Rajandekar and B. Sikdar, "A survey of MAC layer issues and protocols for machine-to-machine communications," *IEEE Internet Things J.*, vol. 2, no. 2, pp. 175–186, Apr. 2015.

[19] J. Peng, H. Tang, P. Hong, and K. Xue, "Stochastic geometry analysis of energy efficiency in heterogeneous network with sleep control," *IEEE Wireless Commun. Lett.*, vol. 2, no. 6, pp. 615–618, Dec. 2013.

[20] T. T. Lam and M. Di Renzo, "On the energy efficiency of heterogeneous cellular networks with renewable energy sources—A stochastic geometry framework," *IEEE Trans. Wireless Commun.*, vol. 19, no. 10, pp. 6752–6770, Oct. 2020.

[21] S. Kaul, R. Yates, and M. Gruteser, "Real-time status: How often should one update?" in *Proc. IEEE INFOCOM*, Orlando, FL, USA, Mar. 2012, pp. 2731–2735.

[22] S. Farazi, A. G. Klein, and D. R. Brown, "Average age of information for status update systems with an energy harvesting server," in *Proc. IEEE INFOCOM Workshop*, Honolulu, HI, USA, Apr. 2018, pp. 112–117.

[23] S. Farazi, A. G. Klein, and D. R. Brown, "Age of information in energy harvesting status update systems: When to preempt in service?" in *Proc. IEEE ISIT*, Vail, CO, USA, Jun. 2018, pp. 2436–2440.

[24] I. Krikidis, "Average age of information in wireless powered sensor networks," *IEEE Wireless Commun. Lett.*, vol. 8, no. 2, pp. 628–631, Apr. 2019.

[25] X. Zheng, S. Zhou, Z. Jiang, and Z. Niu, "Closed-form analysis of non-linear age of information in status updates with an energy harvesting transmitter," *IEEE Trans. Wireless Commun.*, vol. 18, no. 8, pp. 4129–4142, Aug. 2019.

[26] R. D. Yates, "Lazy is timely: Status updates by an energy harvesting source," in *Proc. IEEE ISIT*, Hong Kong, Jun. 2015, pp. 3008–3012.

[27] B. T. Bacinoglu, Y. Sun, E. Uysal, and V. Mutlu, "Optimal status updating with a finite-battery energy harvesting source," *J. Commun. Netw.*, vol. 21, no. 3, pp. 280–294, Jun. 2019.

[28] X. Wu, J. Yang, and J. Wu, "Optimal status update for age of information minimization with an energy harvesting source," *IEEE Trans. Green Commun. Netw.*, vol. 2, no. 1, pp. 193–204, Mar. 2018.

[29] X. Sun, F. Zhao, H. H. Yang, W. Zhan, X. Wang, and T. Q. S. Quek, "Optimizing age of information in random-access poisson networks," *IEEE Internet Things J.*, vol. 9, no. 9, pp. 6816–6829, May 2022.

[30] H. H. Yang, A. Arafa, T. Q. S. Quek, and H. V. Poor, "Optimizing information freshness in wireless networks: A stochastic geometry approach," *IEEE Trans. Mobile Comput.*, vol. 20, no. 6, pp. 2269–2280, Jun. 2021.

[31] M. Emara, H. Elsawy, and G. Bauch, "A spatiotemporal model for peak AoI in uplink IoT networks: Time versus event-triggered traffic," *IEEE Internet Things J.*, vol. 7, no. 8, pp. 6762–6777, Aug. 2020.

[32] P. D. Mankar, Z. Chen, M. A. Abd-Elmagid, N. Pappas, and H. S. Dhillon, "Throughput and age of information in a cellular-based IoT network," *IEEE Trans. Wireless Commun.*, vol. 20, no. 12, pp. 8248–8263, Dec. 2021.

[33] H. H. Yang, A. Arafa, T. Q. S. Quek, and H. V. Poor, "Spatiotemporal analysis for age of information in random access networks under last-Come first-serve with replacement protocol," *IEEE Trans. Wireless Commun.*, vol. 21, no. 4, pp. 2813–2829, Apr. 2022.

[34] P. D. Mankar, M. A. Abd-Elmagid, and H. S. Dhillon, "Spatial distribution of the mean peak age of information in wireless networks," *IEEE Trans. Wireless Commun.*, vol. 20, no. 7, pp. 4465–4479, Jul. 2021.

[35] Y. Chen, S. Zhang, S. Xu, and G. Y. Li, "Fundamental trade-offs on green wireless networks," *IEEE Commun. Mag.*, vol. 49, no. 6, pp. 30–37, Jun. 2011.

[36] R. Mahapatra, Y. Nijsure, G. Kaddoum, N. Ul Hassan, and C. Yuen, "Energy efficiency tradeoff mechanism towards wireless green communication: A survey," *IEEE Commun. Surveys Tuts.*, vol. 18, no. 1, pp. 686–705, 1st Quart., 2016.

[37] S. Zhang, Q. Wu, S. Xu, and G. Y. Li, "Fundamental green tradeoffs: Progresses, challenges, and impacts on 5G networks," *IEEE Commun. Surveys Tuts.*, vol. 19, no. 1, pp. 33–56, 1st Quart., 2017.

[38] J. Gong, X. Chen, and X. Ma, "Energy-age tradeoff in status update communication systems with retransmission," in *Proc. IEEE GLOBECOM*, Abu Dhabi, UAE, Dec. 2018, pp. 1–6.

[39] Y. Gu, H. Chen, Y. Zhou, Y. Li, and B. Vucetic, "Timely status update in Internet of Things monitoring systems: An age-energy tradeoff," *IEEE Internet Things J.*, vol. 6, no. 3, pp. 5324–5335, Jun. 2019.

[40] H. Huang, D. Qiao, and M. C. Gursoy, "Age-energy tradeoff in fading channels with packet-based transmissions," in *Proc. IEEE INFOCOM WKSHPS*, Toronto, ON, Canada, Jul. 2020, pp. 323–328.

[41] S. Nath, J. Wu, and J. Yang, "Optimum energy efficiency and age-of-information tradeoff in multicast scheduling," in *Proc. IEEE ICC*, Kansas City, MO, USA, May 2018, pp. 1–6.

[42] A. Valehi and A. Razi, "Maximizing energy efficiency of cognitive wireless sensor networks with constrained age of information," *IEEE Trans. Cogn. Commun. Netw.*, vol. 3, no. 4, pp. 643–654, Dec. 2017.

[43] Z. Chen, N. Pappas, E. Björnson, and E. G. Larsson, "Optimizing information freshness in a multiple access channel with heterogeneous devices," *IEEE Open J. Commun. Soc.*, vol. 2, pp. 456–470, 2021.

[44] M. Moltafet, M. Leinonen, M. Codreanu, and N. Pappas, "Power minimization for age of information constrained dynamic control in wireless sensor networks," *IEEE Trans. Commun.*, vol. 70, no. 1, pp. 419–432, Jan. 2022.

[45] E. Fountoulakis, N. Pappas, M. Codreanu, and A. Ephremides, "Optimal sampling cost in wireless networks with age of information constraints," in *Proc. IEEE INFOCOM WKSHPS*, Jul. 2020, pp. 918–923.

[46] M. Li, C. Chen, C. Hua, and X. Guan, "Learning-based autonomous scheduling for AoI-aware industrial wireless networks," *IEEE Internet Things J.*, vol. 7, no. 9, pp. 9175–9188, Sep. 2020.

[47] J. Li, D. Wu, C. Yue, Y. Yang, M. Wang, and F. Yuan, "Energy-efficient transmit probability-power control for covert D2D communications with age of information constraints," *IEEE Trans. Veh. Technol.*, vol. 71, no. 9, pp. 9690–9704, Sep. 2022.

[48] *Smart Grid Traffic Behaviour Discussion*, 3GPP document RAN2#69b, R2 102340, Verizon, New York, NY, USA, Apr. 2020.

[49] R. M. Corless, G. H. Gonnet, D. E. Hare, D. J. Jeffrey, and D. E. Knuth, "On the Lambert W Function," *Adv. Comput. Math.*, vol. 5, no. 1, pp. 329–359, 1996.

**Fangming Zhao** received the B.E. degree in communication engineering from the School of Information Engineering, Guangdong University of Technology, Guangzhou, China, in 2019, and the M.S. degree in information and communication engineering from the School of Electronics and Communication Engineering, Sun Yat-sen University (Shenzhen Campus), Shenzhen, China, in 2022. His research interests include age of information, queueing theory, and stochastic modeling of wireless network.

**Xinghua Sun** (Member, IEEE) received the B.S. degree from the Nanjing University of Posts and Telecommunications (NJUPT), China, in 2008, and the Ph.D. degree from the City University of Hong Kong (CityU), China, in 2013. In 2010, he was a visiting student with the National Institute for Research in Digital Science and Technology, France. In 2013, he was a Postdoctoral Fellow with CityU. From 2015 to 2016, he was a Postdoctoral Fellow with the University of British Columbia, Canada. From 2014 to 2018, he was an Associate Professor with NJUPT. Since 2018, he has been an Associate Professor with Sun Yat-sen University, China. From July to August 2019, he was a Visiting Scholar with the Singapore University of Technology and Design, Singapore. His research interests are in the area of stochastic modeling of wireless networks and machine learning for networking. He served as the Technical Program Committee Member for numerous IEEE conferences.

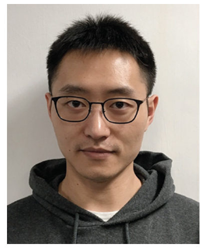

**Wen Zhan** (Member, IEEE) received the B.S. and M.S. degrees from the University of Electronic Science and Technology of China, China, in 2012 and 2015, respectively, and the Ph.D. degree from the City University of Hong Kong, China, in 2019, where he was a Research Assistant and a Postdoctoral Fellow. Since 2020, he has been with the School of Electronics and Communication Engineering, Sun Yat-sen University, China, where he is currently an Assistant Professor. His research interests include Internet of Things, modeling, and performance optimization of next-generation mobile communication systems.

**Xijun Wang** (Member, IEEE) received the B.S. degree (High Hons.) in communications engineering from Xidian University, Xi'an, Shaanxi, China, in 2005, and the Ph.D. degree in electronic engineering from Tsinghua University, Beijing, China, in January 2012. He was an Assistant Professor from 2012 to 2015 and an Associate Professor from 2015 to 2018 with the School of Telecommunications Engineering, Xidian University. From 2015 to 2016, he was a Postdoctoral Research Fellow with the Information Systems Technology and Design Pillar, Singapore University of Technology and Design. He is currently an Associate Professor with Sun Yat-sen University. His current research interests include age of information, edge computing, and Internet of Things. He was a recipient of the Best Paper Award from the IEEE ICCC 2013. He was recognized as an Exemplary Reviewer of the IEEE WIRELESS COMMUNICATIONS LETTERS in 2014.

**Jie Gong** (Member, IEEE) received the B.S. and Ph.D. degrees from the Department of Electronic Engineering in Tsinghua University, Beijing, China, in 2008 and 2013, respectively. From July 2012 to January 2013, he visited The University of Edinburgh, Edinburgh, U.K. From July 2013 to October 2015, he worked as a Postdoctoral Scholar with Tsinghua University. He is currently an Associate Professor with the School of Computer Science and Engineering, Sun Yat-sen University, Guangzhou, China. His research interests include age of information, reinforcement learning, mobile edge computing, and green communications and networking. He was a co-recipient of the Best Paper Award from IEEE Communications Society Asia-Pacific Board in 2013 and the Best Paper Award of the 5th EAI International Conference on IoT as a Service in 2019. He is serving as an Editor for IEEE TRANSACTIONS ON GREEN COMMUNICATIONS AND NETWORKING, IEEE/CIC ICCC 2022 Workshop Co-Chair and has been the Publicity Co-chair for Workshop on Intelligent Computing and Caching at the Network Edge in IEEE WCNC since 2018.

**Xiang Chen** (Member, IEEE) received the B.E. and Ph.D. degrees from the Department of Electronic Engineering, Tsinghua University, Beijing, China, in 2002 and 2008, respectively. From July 2008 to July 2012, he was with Wireless and Mobile Communication Technology Research and Development Center, Research Institute of Information Technology, Tsinghua University. From August 2012 to December 2014, he was with Tsinghua Space Center, School of Aerospace, Tsinghua University. Since January 2015, he has been an Associate Professor with the School of Electronics and Information Technology, Sun Yat-sen University, Guangzhou, China. He is also with Research Institute of Tsinghua University, Shenzhen, as a Chief Researcher (part-time). His research interests mainly focus on 5G wireless communications, wireless big data, Internet of Things, and software radio.